EasyChair Preprint

№ 9454

Aerothrmodynamic Analysis of Inlet Air Temperature Changes Effects on Aero Engines Performance and Aero Engines Optimization for High Speeds and High Altitudes Flight Conditions

Mohamadreza Sabzehali and Mahdi Alibeigi

December 11, 2022

AEROTHRMODYNAMIC ANALYSIS OF INLET AIR TEMPERATURE CHANGES EFFECTS ON AERO ENGINES PERFORMANCE AND AERO ENGINES OPTIMIZATION FOR HIGH SPEEDS AND HIGH ALTITDUES FLIGHTCONDITIONS

M.Sabzehali, M. Alibeigi

Abstract

In this study, the effect of inlet air and Mach and flight height variations on the performance of XRJ47-5 ramjet air engines, F135PW100 and EJ200 turbofan engines, and J85 GE17 turbojet engines have been investigated. Thrust and specific fuel consumption (TSFC) and fuel consumption, thermal and thrust efficiencies, and the intensity of nitrogen emissions (I nox) and the actual flow of air entering the engine are considered as performance. At an altitude of 10,000 meters in Borazi, 8 for 20 in the directions and 317 0, the inlet air relative to I Standard Atmosphere (International) for Terabufen F135PW100 and EJ2, 0% and Turbojet J85 GE1, Trust Force and 112 to 3.5 degrees, 7.5%, 0.96% and 0.23% It has been reduced by using the female algorithm used to optimize the engines of the study in the altitude range of 20000-40000 meters and Mach 2-4.5.

Key words F135PW100, RAMJET, OPTIMIZATION, HIGHT ALTITUDE,SUPERSONIC

INTRODUCTION

Gas turbines are a type of power generation cycle. The gas turbine engine is an internal combustion engine of the rotating machine type. These engines operate based on the Bratton cycle. Gas turbines are widely used in various industries such as oil and gas and petroleum. They have electric energy production plants and aircraft propulsion systems. The simplest configuration of air gas turbine engines is the turbojet engine. In a turbojet, the air first enters the compressor and is condensed, then it enters the penetration chamber, and the temperature and enthalpy increase from the reaction with the fuel. It then enters the turbine and the temperature and pressure It decreases. The turbine provides the mechanical power required by the compressor. The gases from the combustion of fuel and air enter the nozzle after exiting the turbine. The nozzle expands and the flow rate increases, then it is discharged into the environment. As a result of the reaction caused by the discharge of the turbine output flow to the environment, the thrust force was produced according to the speed and pressure of the flow at the nozzle outlet and the pressure of the environment.[1] Another type of air gas turbine engines is a turbofan engine. The main difference between a turbofan engine and a turbojet engine is the presence of an axial fan located above the compressor and a nozzle on the side of the passage for a part of the incoming air flow. Enmix are divided. . The main components of the turbofan engine are the turbofan, the mixing flow, the axial flow fan, the compressor, the combustion chamber, the turbine, the mixer, and the nozzle. The air flow entering the engine is divided into the cold flow after passing through the fan. The hot flow enters the compressor and condenses. Hot enters the turbine and its temperature and pressure decrease. The pulp enters the mixer, it is mixed with the cold (bypass) flow in the mixer, and the pulp is discharged into the environment

through the nozzle. As a result of the reaction caused by the discharge of the turbine output flow to the environment, the thrust force was produced according to the speed and pressure of the flow at the nozzle outlet, as well as the pressure of the environment. [2]

Another type of air-breathing combustion engines are ramjets. Ramjet engines work like gas turbine engines based on the Brayton cycle, with the difference that in ramjet engines, due to the high Mach of the incoming air flow, the entire compression process is performed in the intake and diffuser in the form of aerodynamic compression. Therefore, in these engines, there is a lack of rotating components. In these engines, first the air flow with high Mach enters the intake, then it condenses and heats up in the intake and diffuser, then it enters the burner and reacts with the fuel. Enough of that in the expanded nozzle. and the speed of the flow increases. It is discharged to the environment. As a result of the reaction of the discharge of the current to the environment, thrust force is created. [3] The results of the thermodynamic analysis of the performance of a gas turbine power plant show that the compression ratio and the ambient air temperature have a great impact on the thermal efficiency as much as the isenerobic efficiencies. So that the thermal efficiency and the output power decrease directly with the increase in the ambient air temperature. Also, the specific fuel consumption And the heating rate increases directly with the increase in ambient air temperature. (M. Rahman et al, 2011) [4]. Thermodynamic analysis and thermodynamic optimization of gas turbines as turbojet superchargers have been carried out. It has been observed that specific thrust is strongly dependent on TIT, so that a 10% reduction in TIT leads to a 6.7% reduction in specific thrust and a 6.8% reduction in specific consumption. Also, the optimal values for turbojets are 13,000 meters' altitude, 0.8 Mach, compression ratio 14, and TIT 1700 Kelvin (Najjar and Balaneh 2015). [5]. Also, optimization of the performance of a gas micro turbine has been done with the aim of maximizing the specific thrust and minimizing the specific fuel consumption. The results of this study show that the specific fuel consumption and specific thrust of the turbojet engine is highly dependent on the TIT and the compression ratio of the compressor. (Swe et al,2018) The efficiency of 0.3 to 0.8 was investigated. The results showed that in the range of Mach 0.3 to 0.8, the exhaust efficiency ranges from 48.61 to 49.88 and the energy efficiency varies from 3.25 to 9.96%. Also, the exhaust efficiency for the compressor from the center is 61.11% and for the combustion chamber is 89.21%. And for the turbine, it has been evaluated at 84.11%. Also, at a constant altitude, the exergy efficiency and energy efficiency of the engine both increase with the increase of Mach number. (Turan, 2018) [7] Also in another study, optimization with PSO algorithm based on Turbocharged engine J85 GE21 has been carried out in the altitude range of 1000 to 8000 meters and the air velocity is 200 m/s. In this study, the compression ratio of the compressor, the air flow Mach number and the isentropic efficiencies of the turbine nozzle and the compressor were considered as design parameters. The highest exergy efficiency among the engine components in different conditions was calculated as 73.1% for the diffuser. (Ahmadi Nasab and Ehyaei, 2019) This code is able to calculate the data of thermodynamic cycles with an error of 0.03% compared to the results obtained from the NPSS program (Hendricks and Gray, 2019) [9]. Zentic algorithm has been done. Also in this study, TurboJet-Engine Optimizer v1 program was used to calculate the thermodynamic characteristics of the engine and optimize it (Tia et al, 2012) [10]. Various J85 GE21 turbojet engines for us The values of 0.4, 0.6 and 0.8 have been taken. In this study, in order to find the main parameters affecting the efficiency, barometric analysis was done based on

exergy analysis. In the study, it was observed that TSFC increases with increasing Mach number. (Bastani et al, 2015)[11]. Also in Another study has been carried out to investigate the economic performance of a turbojet engine in the state of its design area. In this study, the exhaust efficiency was calculated as 50.13% (Sohret, 2018) [12]. Also, optimization of a gas turbine power cycle with functions The objective of maximizing the thermal efficiency is maximizing the net power output and minimizing the engine speed with the design variables of the compressor compression ratio, the turbine inlet temperature, the ambient air temperature (Nikaein, 2011)[13]. In another study, the effect of the bypass ratio on the optimal fan pressure ratio It has been studied in a turbofan engine. In this study, the Trent XBW series engine was investigated. The results of this study show that increasing the bypass ratio reduces specific fuel consumption and increases thrust. (Xue et al, 2019)[14]. Also, in another paper, a barometric study The turbofan engine is built with high pressure bypass. (Asundi and Firasat Ali, 2019) (Jakubowski, 2019) [16]. Also, in another case, it is applied to the aerodynamic analysis of mixed flow turbofan engines..... (Khalid, 2017) [17]. Also, in another study, compressor compression ratio, fan pressure ratio, and turbine outlet temperature were investigated on the performance of the mixed flow turbofan engine.

Also, in another study, compressor compression ratio, fan pressure ratio, and turbine outlet temperature were investigated on the performance of a mixed flow turbofan engine (Jakubowski, 2009) [18]. (Cleary, 2018) [19]. In another study, the performance of turbojet and turbofan engines and variable cycles for high speed engines was investigated. And the height of the Beruri Trust and the specific fuel consumption of Turjet and Turbofan engines have been investigated (Kurzke, 2018) [20]. In another study, a thermodynamic analysis of a turbofan engine using hydrogen as fuel has been done. The results of this study showed that using hydrogen fuel instead of fossil fuels leads to an increase in specific thrust and a decrease in specific fuel consumption under equal conditions. Marszalek, 2018 [21]. In another study, the thermodynamic cycle of a turbofan engine was optimized. In this study, the optimization was done with the aim of minimizing specific fuel consumption and with four objective functions: bypass ratio, total compression ratio, fan compression ratio and turbine inlet temperature. The results of this study show increasing the turbine inlet temperature as well as increasing the overall compression ratio leads to an increase in thrust and a decrease in specific fuel consumption. Also, with an increase in the bypass ratio, thrust and specific fuel consumption both decrease. (Najjar and Al-Sharif, 2006) [22] Another article deals with the conceptual design and optimization of a turbofan engine for commercial supersonic jets (Nordqvist et al, 2017) [23]. The results of this study showed that with an increase in the overall pressure ratio, the overall efficiency and thermal efficiency increase and the propulsion efficiency decreases. Also, with the increase in the inlet temperature of the turbine, the specific fuel consumption and the specific thrust increase. Also, with the increase in the fan compression ratio, the specific consumption decreases. and the special trust increases, and with the increase of the bypass ratio, the special trust decreases and so on The overall performance increases. (EI-Sayed and Emeara, 2018) 3.5 and the flight height of 12,000 meters has been calculated. Another study was conducted to investigate the thermodynamic efficiency and thrust of air-breathing jet engines with combustion in the subsonic regime (Kraiko and Egoryan, 2018) [27]. This study has investigated the effect of inlet air temperature variations on compressor efficiency. (Ibrahim et al, 2018) [29]. In another study, the

exhaust analysis of GE-F5 gas turbine engine with inlet air cooling was carried out. In this study, simulation was done using MATLAB software. The results of this study It shows that for each degree Celsius decrease in the inlet air temperature in the range of 14 to 50 degrees Celsius, the thermal efficiency and output power increased by 0.085% and 0.16 MW, respectively. (Arabi et al, 2019) [30]. 2 3 In this study, firstly, the effect of temperature changes in the inlet air to mixed flow turbofan and ramjet turbojet engines at different Machs and cruising altitudes was investigated, and based on the results of this investigation and the results of other similar studies, the optimization of engines with different target functions was carried out. . Considering the operational advantages of flying at high altitudes and also the decrease in ambient air density with the increase in altitude, which leads to a decrease in the dynamic pressure of air flow at any fixed speed, in this study, firstly, the thermodynamic cycle of Gianmix turbofan engines with Bayin F135PW100, EJ200 by-pass ratio J85 GE21 turbojet engine and XRJ47-W-5 ramjet engine were modeled with GASTURB 10 software and the modeling results were validated with references. Sebs was optimized with Zentic algorithm and MATLAB 10 software in two phases and in each phase for 3 separate objective functions. Sebs were selected with Tabsys algorithm for two approaches from the optimized cycles based on J85 GE21 turbojet engines and F135PW100, EJ200 engines in two phases of designing the best cycles. 3.

1- موتور F135PW100

F135 PW100 engine is a two-shaft mixed flow turbofan engine with a by-basin ratio with the ability to burn. The main components of this engine include three layers of axial flow fan, 6 layers of axial flow compressor, annular type combustion chamber with one layer of high pressure axial flow turbine and two layers of turbine. The weak pressure is the axial flow and the nozzle. This engine is a product of PRATT AND WHITNEY company and it is used as the propulsion system of the LOCKHEED MARTIN-F35 LIGHTNING aircraft. In this study, the non-burner version of this engine was considered. [4] The schematic of the F135 PW100 engine is shown in Fig. 4

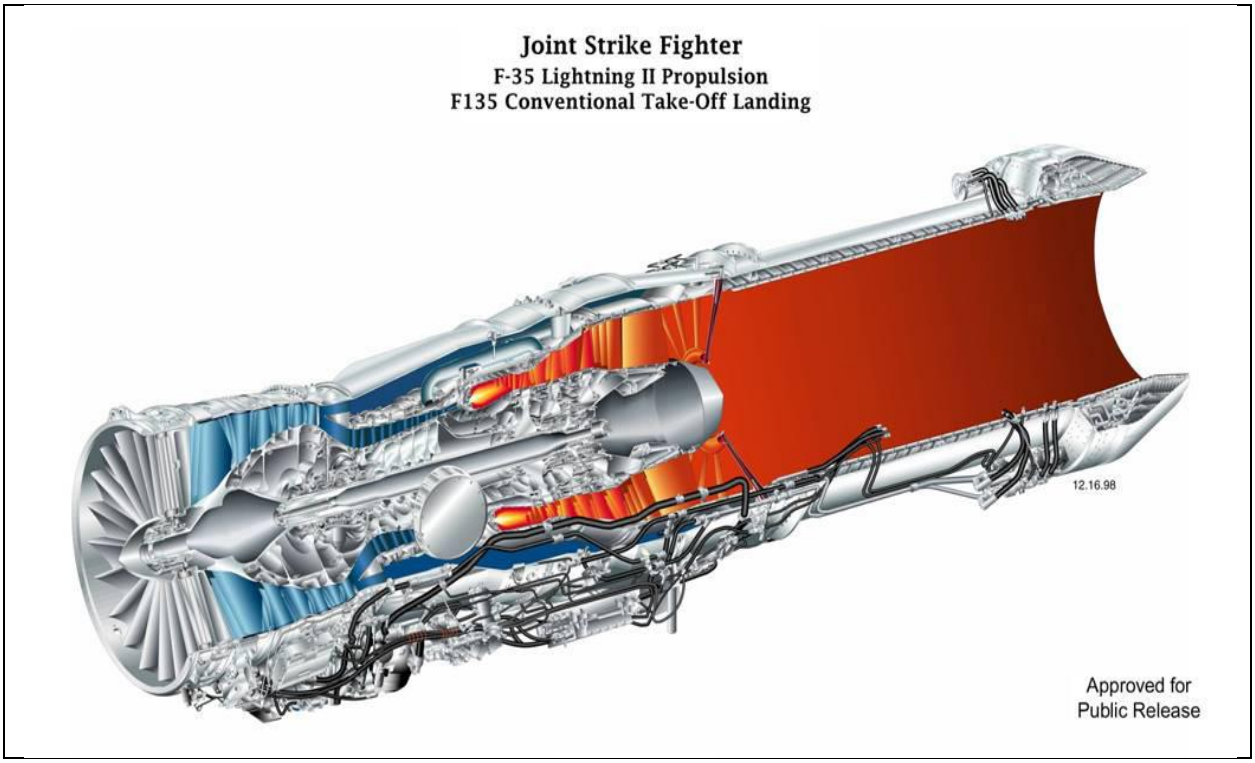

Schematic diagram of F135 PW100 engine []

2-Engine EJ200

6 EJ200 engine is a turbofan engine with two shafts of mixing flow with a by-pass ratio and a combustion capability. Its main components include three layers of axial flow fan, 5 layers of axial flow compressor, annular type combustion chamber with 3 layers of high pressure axial flow turbine and 5 The low pressure turbine floor is axial flow and nozzle. This engine is a product of AERO JET TURBO GMBH company and it is used as the thrust system of EUROFIGHTER TYPHOON aircraft. [] The schematic of the EJ200 engine is shown in figure (). 6

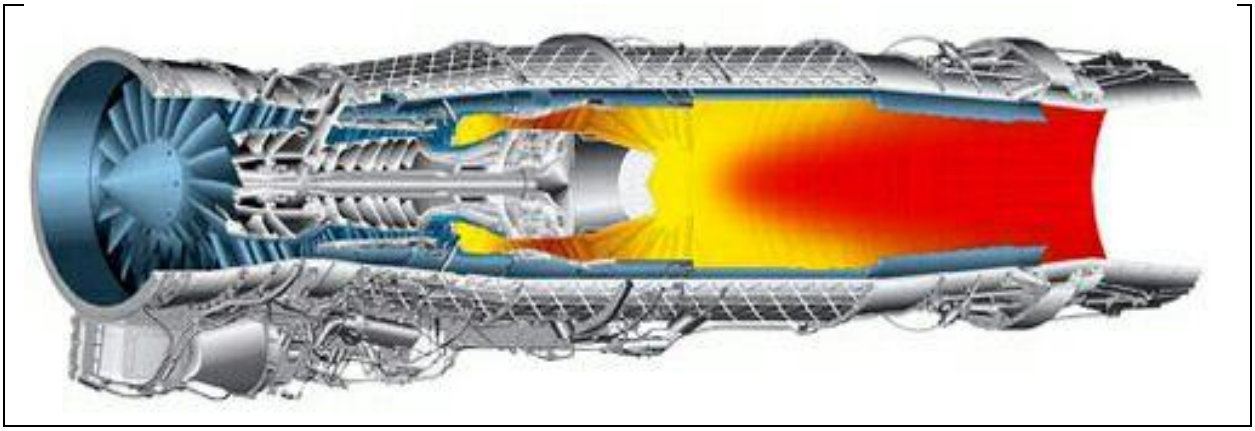

Schematic diagram of EJ engine []

3-Engine J85 GE17

J85 GE17 is a single shaft turbojet engine. Its main components include an 8-stage axial flow compressor, a 2-stage axial flow turbine, and an annular combustion chamber and nozzle. This engine is a product of General Electric Company and has been used as an engine for Northrop F5 aircraft. [] 7

4- XRJ47-W-5 engine

XRJ47-W-5 is an American ramjet engine made by Wright Aeronautical Company. This engine is used as a high-speed system for the Kuroz SM64 Navaho missile. 8 []. Schematic cycle of J85GE21 turbojet, F135 PW100 turbofan, EJ200 turbofan, XRJ47-W-5 ramjet engines with intake air cooling system 9. The flow chart of the turbofan engine with the mixing flow with the inlet air cooling system is shown in figure (9).

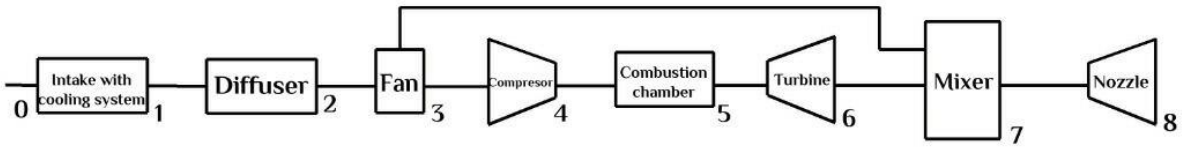

Figure () flow chart of turbofan engine with mixed flow with air intake cooling system 10. The turbojet engine flow chart with the intake air cooling system is shown in Figure (10).

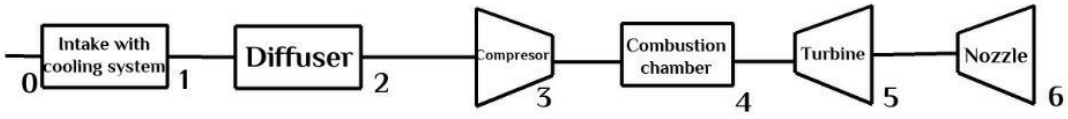

Figure () flow chart of turbojet engine with intake air cooling system The flow diagram of the ramjet engine with the intake air cooling system is shown in figure ().

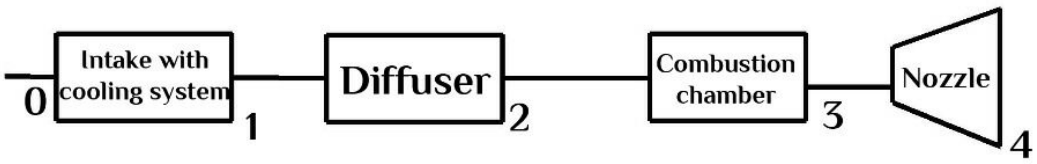

Figure () flow diagram of Ramjet engine with air intake cooling system

In this study, a two-shaft mixed-flow turbofan engine (F135PW100), two-shaft mixed-flow turbofan engine EJ200, single-shaft J85 GE17 engine and XRJ47-W-5 ramjet engine have been investigated. Figure 1 shows a schematic of the studied engines. Figure 2 shows the flow chart of the turbofan engine, the mix flow with the intake air cooling system, the turbojet engine with the intake air cooling system, and the ramjet engine with the intake air cooling system.
Thermodynamic and thermal modeling

1)Turbojet equestations

The changes in air flow pressure at the intake and cooling system is negligible:

$$P_0 = P_1 \quad (1)$$

$$T_1 = T_0 + \Delta T \quad (2)$$

P_0 and T_0, respectively, ambient air pressure and ambient air temperature and P_1 and T_1, respectively, are diffuser inlet pressure and diffuser inlet temperature, P_2 and T_2 , respectively are the fan inlet pressure and fan inlet temperature and ΔT is the temperature difference between diffuser inlet to ambient .

Assuming the diffuser is isentropic, diffuser exit air temperature is calculated as follows.

$$\boldsymbol{T_2 = T_1\left(1 + \frac{k_d - 1}{2} M_a^2\right)} \quad \textbf{(3)}$$

where T_1 and T_2 are exit and inlet air temperature to the diffuser.k_dSpecific heat at constant pressure to specific heat in constant volume for air passing through the diffuser, which is a function of the average temperature of the air passing through flight mach number. M_a is flight mach number. The exiting air pressure of the diffuser is calculated as follows.

$$\boldsymbol{P_2 = P_1\left(\frac{T_2}{T_1}\right)^{\frac{k_d}{k_d - 1}}} \quad \textbf{\textit{(4)}}$$

Where P_1 and P_2 are air pressure at exit and inlet of the diffuser, respectively; and T_1 and T_2 are exit and inlet air temperature to the diffuser. $k_d$specific heat at constant pressure to specific heat in constant volume for passing air of diffuser which is calculated as a function of the average temperature of the passing air of the diffuser. Assuming air and fuel combustion products with air are ideal gas. The compressore exit pressure is obtained from the following equation.

$$P_{3=\pi_c} P_2 \quad (5)$$

π_c is compressor pressure ratio and $P_3$is compressor exit pressure and $P_2$is fan exit air pressure The exit temperature of compressor is obtained as follow

$$T_3 = \frac{T_2}{\eta_C}\left[\left(\frac{P_3}{P_2}\right)^{\frac{k_c - 1}{k_c}} - 1\right] + T_2 \quad (6)$$

Where $\eta_c$is compressor isentropic efficiency and $T_3$is compressor exit air temperature and $T_2$is fan exit air temperature and K_c is specific heat at constant pressure to specific heat in constant volume for passing air of fan is calculated as a function of the average air passing. Engine intake air real mass flow rate is calculated as follow

$m_a = \rho V_0 A$	(7)

Where A is cross section of real air inlet flow and ρ is density of inlet air flow and $V_0$is flight velocity. Flight velocity is calculated in which

$V_0 = M_a(RkT_0)^{0.5}$	(8)

That M_a is the flight mach number, R is the global constant gas, and k is the ratio of specific heat at constant pressure to specific heat at constant valume of air is calculated as a function of the ambient air temperature. V_0 is also the flight velocity

Compressor power is obtained as follows.

$$W_C = m_a \frac{T_2}{\eta_C}\left[\left(\frac{P_3}{P_2}\right)^{\frac{k_c-1}{k_c}} - 1\right] + T_2 \quad (9)$$

WhereW_C is compressor power consumption and $\eta_C$is compressor isentropic efficiency and $K_c$is specific heat at constant pressure to specific heat in constant volume ratio is calculated as a function of the average of compressor air temperature.$m_a$is real air mass flow rate. . Combustion chamber exit pressure is obtained as follow

$$P_4 = P_3 - \Delta P_{combustor} \quad (10)$$

Where $P_4$is combustion chamber exit pressure P_3 is compressor inlet pressure

$\Delta P_{combustor}$ is pressure drop in the combustion chamber is evaluated as a percentage of the air exit pressure of compressor.Heat rate is calculated as follow

$$Q_h = m_a C_{av}(T_4 - T_3) \quad (11)$$

Where Q_h is heat rate and $C_{av}$is specific heat at costant pressure is calculated as a function of average flow temperature in the combustion chamber.also $T_3$is inlet air temperature of turbine and $T_4$is inlet air temperature of turbine.Fule mass flow rate is calculated as follow

$$m_f = \frac{Q_h}{FHV\ \eta_{combustor}} \quad (12)$$

Where FHVis fuel heat value per kilograms and $\eta_{combustor}$is combustion efficiency at combustion chamber and m_f is fuel consumption and $Q_h$is heat rate.Turbine intake mass flow rate is calculated as follow

$$m_T = m_a + m_f \quad (13)$$

Where $m_f$is fuel consumption rate and $m_a$is real air mass flow rate.

Turbine power is calculated as follow

$$W_T = m_T . C_{Pavt} . (T_4 - T_5) \quad (14)$$

Where $m_T$is turbine inlet mass flow rate and $C_{pav}$is specific heat at costant pressure which is obtained as a function of the average temperature in the turbine.

Assuming that mechanical power losses in the spools is negligible, according to the energy conservation law, the turbine power is equal to the compressor power

$$m_T.C_{Pavt}.(T_5 - T_6) = m_a\left[\frac{T_2}{\eta_C}\left[\left(\frac{P_3}{P_2}\right)^{\frac{k_c-1}{k_c}} - 1\right] + T_2\right] \quad (15)$$

In which T_5 is the turbine exit temperature and T_4 is the turbine inlet temperature, m_T is the turbine mass flow rate and C_{pavt} is the specific heat at costant pressure, which is obtained as a function of the average temperature during the turbine. η_c is also the compressor isentropic efficiency. Also, k_c is the ratio of *specific heat at costant* pressure to specific heat of the same volume as air, which is calculated as a function of the average air temperature during compressor. By obtaining the turbine exit temperature of the equation (17), the turbine exit pressure is calculated as follows:

$$\boldsymbol{P_5 = P_4\left[1 - \frac{1}{\eta_t}\left(1 - \frac{T_5}{T_4}\right)\right]^{\frac{k_t}{k_t-1}}} \quad \textbf{(16)}$$

T_5 is the output temperature of the turbine, T_4 is the inlet temperature of the turbine, and $P_5$and P_4 , respectively , are the turbine exit pressure and turbine inlet pressure. k_t is the ratio of specific heat at costant pressure to specific heat at constant valume, which is a function of the average temperature during the turbine, and η_T is the turbine isentropic efficiency.

The flow pressure at the nozzle exit is obtained

$$P_6 = P_5\left[1 - \frac{1}{\eta_n}\left(1 - \left(\frac{T_6}{T_5}\right)\right)\right]^{\frac{K_n}{K_n-1}} \quad (17)$$

that P_6 is the flow pressure at the output nozzle and T_6 is the flow temperature at the output nozzle and Kn is the ratio of specific heat at costant pressure to hot stream nozzle exit ,Which is obtained as a function of the average temperature along the stream nozzle and $\eta_n$is the nozzle isentropic efficiency.

The nozzle exit velocity is obtained in such a way

$$V_6 = \left(2\eta_n \frac{K_n}{K_n - 1}.R.T_6\left[1 - \left(\frac{P_6}{P_5}\right)^{\frac{K_n-1}{K_n}}\right]\right)^{0.5} \quad (18)$$

that K_n is the ratio of specific heat at cost constant pressure to specific heat at constant valume, which is a function of the average temperature during nozzle and R is the global gas constant, P_7 is the nozzle exit pressure. thrust is calculated in such a way

$$F = \frac{1}{g_c}\left[\left((m_a + m_f)(V_6)\right) - (m_a V_0)\right] + [A_6(P_6 - P_0)] \quad (19)$$

that A_6 is the nozzle exit area, P_0 is the ambient air pressure, V_0 is the flight speed, and g_c is the gravity of the earth and F is the thrust force, and m_a is the real air mass flow rate. The specific fuel consumption is equal to the ratio of fuel mass flow rate to thrust force,

$$TSFC = \frac{m_f}{F} \quad (20)$$

in which TSFC is the specific fuel consumption. Thermal efficiency is calculated in such a way

$$\eta_{th} = \frac{m_T(V_6^2 - V_0^2)}{2m_f FHV} \quad (21)$$

that $\eta_{th}$is the thermal efficiency of the engine and m_T is the turbine exit mass flow rate. Propulsive efficiency is calculated in such a way

$$\eta_P = \frac{V_0 F}{m_T(V_6^2 - V_0^2)} \quad (22)$$

that η_P is the propulsion efficiency of the engine and m_T is the mass flow rate.

2)Mixed flow turbofan equestaion

The thermodynamic and thermal modeling equations of the mixing flow turbofan are shown in Table (). 11

Table () of thermodynamic and thermal modeling equations of mix flow turbofan

$P_0 = P_1$ $T_1 = T_0 + \Delta T$	$W_T = m_T . C_{Pavt} . (T_5 - T_6)$
$\boldsymbol{T_2 = T_1\left(1 + \frac{k_d - 1}{2} M_a^2\right)}$	$\boldsymbol{P_6 = P_5\left[1 - \frac{1}{\eta_t}\left(1 - \frac{T_6}{T_5}\right)\right]^{\frac{k_t}{k_t - 1}}}$
$P_{3=\pi_{fan}} P_2$	$T_7 = \frac{T_6 C_{P6} m_{ah} + (m_{ac} C_{P3} T_3)}{C_{P7}}$
$T_3 = \frac{T_2}{\eta_{fan}}\left[\left(\frac{P_3}{P_2}\right)^{\frac{k_f - 1}{k_f}} - 1\right] + T_2$	$P_7 = RT_7$
$P_{4=\pi_c} P_3$	$m_7 = m_{ah} + m_{ac} + m_f$

$T_4 = \frac{T_3}{\eta_C}\left[\left(\frac{P_4}{P_3}\right)^{\frac{k_c-1}{k_c}} - 1\right] + T_3$	$P_8 = P_7\left[1 - \frac{1}{\eta_n}\left(1 - \left(\frac{T_8}{T_7}\right)\right)\right]^{\frac{K_n}{K_n-1}}$
$m_{total} = \rho V_0 A$	$V_8 = \left(2\eta_n \frac{K_n}{K_n - 1} R T_7 \left[1 - \left(\frac{P_8}{P_7}\right)^{\frac{K_n-1}{K_n}}\right]\right)^{0.5}$
$m_{ah} = \frac{m_{total}}{\alpha + 1}$	$F = m_7(V_8 - V_0) + A_8(P_8 - P_0)$
$W_C = m_{ah}\frac{T_3}{\eta_C}\left[\left(\frac{P_4}{P_3}\right)^{\frac{k_c-1}{k_c}} - 1\right]$	$TSFC = \frac{m_f}{F}$
$W_{fan} = m_{ac}\frac{T_2}{\eta_{fan}}\left[\left(\frac{P_3}{P_2}\right)^{\frac{k_f-1}{k_f}} - 1\right]$	$\eta_{th} = \frac{m_7(V_8^2 - V_0^2)}{2m_f FHV}$
$m_{ac} = m_{total} - m_{ah}$	$\eta_P = \frac{V_0 F}{m_7(V_8^2 - V_0^2)}$
$P_5 = P_4 - \Delta P_{cambustor}$	
$Q_h = m_{ah} C_{av}(T_5 - T_4)$	
$m_f = \frac{Q_h}{FHV\ \eta_{combustor}}$	
$m_T = m_{ah} + m_f$	

12 where m_total is the mass flow rate of the incoming air, and m_ah and m_ac are the mass flow rate of the incoming air to the compressor and the mass flow rate of the copper bypass air, respectively. Also, ρ, V_0 and A are the parameters of the ambient air density, the speed of the engine and the cross section of the air inlet channel of the engine. Also, α is the bypass ratio of the engine. π_fan and η_fan respectively pressure ratio. is the overall compressor and the isentropic efficiency of the fan. Also, π_C and η_C are the ratio of the overall pressure of the compressor and the isentropic efficiency of the compressor, respectively. Also, T_4 is the temperature of the burner outlet flow. Also, T_7 and P_7 are the pressure and temperature of the flow at the mixer outlet, and T_8 and P_8 are The order of temperature and flow pressure is at the outlet of the nozzle. 12

3) Ramjet equations

The changes in air flow pressure at the intake and cooling system is negligible:

$P_0 = P_1$	(23)
$T_1 = T_0 + \Delta T$	(24)

P_0 and T_0, respectively, ambient air pressure and ambient air temperature and P_1 and T_1, respectively, are diffuser inlet pressure and diffuser inlet temperature, P_2 and T_2 , respectively are the fan inlet pressure and fan inlet temperature and ΔT is the temperature difference between diffuser inlet to ambient .

Assuming the diffuser is isentropic, diffuser exit air temperature is calculated as follows.

$$\boldsymbol{T_2 = T_1\left(1 + \frac{k_d - 1}{2} M_a^2\right)}$$	**(25)**

where T_1 and T_2 are exit and inlet air temperature to the diffuser.k_dSpecific heat at constant pressure to specific heat in constant volume for air passing through the diffuser, which is a function of the average temperature of the air passing through flight mach number. M_a is flight mach number. The exiting air pressure of the diffuser is calculated as follows.

$$\boldsymbol{P_2 = P_1\left(\frac{T_2}{T_1}\right)^{\frac{k_d}{k_d - 1}}}$$	***(26)***

Where P_1 and P_2 are air pressure at exit and inlet of the diffuser, respectively; and T_1 and T_2 are exit and inlet air temperature to the diffuser. $k_d$specific heat at constant pressure to specific heat in constant volume for passing air of diffuser which is calculated as a function of the average temperature of the passing air of the diffuser. Assuming air and fuel combustion products with air are ideal gas. Combustion chamber exit pressure is obtained as follow

$$P_3 = P_2 - \Delta P_{combustor} \quad (26)$$

Where $P_3$is combustion chamber exit pressure P_2 is compressor inlet pressure

$\Delta P_{combustor}$ is pressure drop in the combustion chamber. Heat rate is calculated as follow

$$Q_h = m_a C_{av}(T_3 - T_2) \quad (27)$$

Where Q_h is heat rate and $C_{av}$is specific heat at costant pressure is calculated as a function of average flow temperature in the combustion chamber.also $T_2$is inlet air temperature of turbine and $T_3$is inlet air temperature of nozzle .Fule mass flow rate is calculated as follow

$$m_f = \frac{Q_h}{FHV\ \eta_{combustor}} \quad (28)$$

Where FHVis fuel heat value per kilograms and $\eta_{combustor}$is combustion efficiency at combustion chamber and m_f is fuel consumption and $Q_h$is heat rate.nozzle inlet mass flow rate is calculated as follow

$$m_T = m_a + m_f \tag{28}$$

Where m_f is fuel consumption rate and m_a is hot stream real air mass flow rate. The flow pressure at the nozzle exit is obtained

$$P_4 = P_3 \left[1 - \frac{1}{\eta_n}\left(1 - \left(\frac{T_4}{T_3}\right)\right)\right]^{\frac{K_n}{K_n - 1}} \tag{29}$$

that P_4 is the flow pressure at the output nozzle and T_4 is the flow temperature at the output nozzle and Kn is the ratio of specific heat at costant pressure to nozzle exit ,Which is obtained as a function of the average temperature along the nozzle and η_n is the nozzle isentropic efficiency.

The nozzle exit velocity is obtained in such a way

$$V_4 = \left(2\eta_n \frac{K_n}{K_n - 1}.R.T_4\left[1 - \left(\frac{P_4}{P_3}\right)^{\frac{K_n - 1}{K_n}}\right]\right)^{0.5} \tag{29}$$

that K_n is the ratio of specific heat at cost constant pressure to specific heat at constant valume, which is a function of the average temperature during nozzle and R is the global gas constant, P_4 is the nozzle exit pressure. thrust is calculated in such a way

$$F \quad = \frac{1}{g_c}\left[\left((m_a + m_f)(V_4)\right) - (m_a V_0)\right] + [A_4(P_4 - P_0)] \tag{30}$$

that A_6 is the nozzle exit area, P_0 is the ambient air pressure, V_0 is the flight speed, and g_c is the gravity of the earth and F is the thrust force, and m_a is the real air mass flow rate. The specific fuel consumption is equal to the ratio of fuel mass flow rate to thrust force,

$$TSFC = \frac{m_f}{F} \tag{31}$$

in which TSFC is the specific fuel consumption.

. Propulsive efficiency is calculated in such a way

$$\eta_P = \frac{V_0 F}{m_T(V_4^2 - V_0^2)} \tag{32}$$

that η_P is the propulsion efficiency of the engine and m_T is the mass flow rate.

TSF is calculated in such a way

$=\frac{F}{m_{total}} TSF$	(33)

That F is thrust force andm_{total} is intake real air mass flow rate

Another parameter called Cd ratio as a measure of engine acceleration ability is equal to the thrust force ratio to the dynamic pressure of the air flow around the aircraft.

$Cd = \frac{2F}{\rho_0 \, V_0^2}$	(34)

where ρ_0^ is the ambient air density and V_0 is the flight speed and F is the thrust force. 14For turbine engines the nitrogen oxides emission index coefficient (snox) is obtained in such a way

$$S_{nox} = (\frac{P_4}{2965kPa})^{0.4} e^{(\frac{T_4 - 826K}{194K} + \frac{6.29 - (100.war)}{53.2})} \quad (35)$$

that T_4 and P_4, respectively, are the compressor exit air temperature and compressor exit air pressure and war is the ratio of liquid water air to the compressor exit air. In this study, the effect of fuel type and combustor geometry on the index of production intensity of snox has been omitted and only the effect of temperature, pressure and liquid water air ratio of the incoming air on it has been discussed.

Also, the parameter of the emission coefficient of nitrogen oxides EI nox is calculated as follows;

EI nox=23Snox	(36)

where EE nox is the emission parameter of nitrogen oxides

Table 1 of input parameters for engines based on references[]

	F135 PW 100 turbofan	EJ200 turbofan	J85 GE17 turbojet
$T_{inlet\ turbine}$	2175(K)	1800(K)	1139(K)
Overall compressor pressure ratio	28.2	26	7
$Fan\ pressure\ ratio$	5.1	4.2	-
$Bypass\ ratio$	0.57	0.4	-
$\dot{m}_{air}$	147(Kg/s)	77(Kg/s)	20(Kg/s)
$\eta_{is,fan}$	0.90	0.90	0.87
$\eta_{is,compressor}$	0.85	0.85	0.9

Table(). Thermodynamic cycle input parameters of three engines F135PW100, EJ200, J85 GE21

Parameters	Values
Burner exit temperature	2300(K)
Burner inlet Mach number	0.2
Air mass flow rate	55(Kg/s)

$\eta_{is,nozzle}$	0.92

Table(). Thermodynamic cycle input parameters of XRJ47-W5 engine.

Table (calorific value of considered fuels).

The Fuel heat value, table of considered fuels [16-21]			
Fuel heat value	hydrogen	Natural gas	Jp10
	118(Mj/kg)	49.736(Mj/kg)	42.076(Mj/Kg)

Validation 16

In this study, GASTURB10 software was used to model the thermodynamic cycle. Cycle parameters of EJ200, F135 PE100, J85GE17 engines are in the engine table. XRJ47-W-5 is shown in table () and the calorific value of fuels is shown in table (). In order to validate the modeling, the values calculated for thrust and TSFC for F135PW100, EJ200, J85 GE17 engines in tick mode F (Ma=0, H=0) and for the XRJ47-W-5 engine in the state (Ma=2.75, H=18333m) for JP10 fuel, we have compared with the reference values. Thrust and TSFC values of F135PW100, EJ200, J85 engines GE17 in tick-off state (Ma=0, H=0) of XRJ47-W-5 engine in (Ma= , H=) for JP10 fuel compared to the reference values in table () is displayed. The difference percentage of the results for Trust Force is in the range of 12.33-2.97% and for TSFC in the range of 8-4.22%. 16

Table (comparison of trust force and TSFC with references in take-off mode).					
		F135PW100	EJ200	J85 GE17	XRJ47-W-5
$Thrust(KN)$	$Reference\ value$	125.90[].	60[]	[]12.67	45[]
	$Present\ study$	122.16	63.28	12.52	39.45
	$diveation(\%)$	-2.97	5.46	1.18	12.33
$TSFC(g/KNs)$	$Reference\ value$	25[]	23[]	27[]	95[]
	$Present\ study$	27	23.971	23.733	87.507
	$diveation(\%)$	8	4.22	8.71	7.88

Results 17 In this part, by using thermodynamic modeling, the effect of temperature changes in the inlet air to mixed flow turbofan and ramjet turbojet engines at different Mach and altitudes has been investigated. 17 1-Effect of mach number and flight altitude on aero engine performance and real air mass flow rate effect 18 Measurements of the actual flow rate of the inlet air to the engine and thrust of the J85GE21 turbojet, F135 PW100 turbofan, EJ200 turbofan engines at an altitude of 20,000 meters and a Mach range of 0.5 to 2.5 and XRJ47-W-5 engine at an altitude of 20,000 meters and a Mach range of 2.5 to 4 For JP10 fuel, it is shown in figure (18).

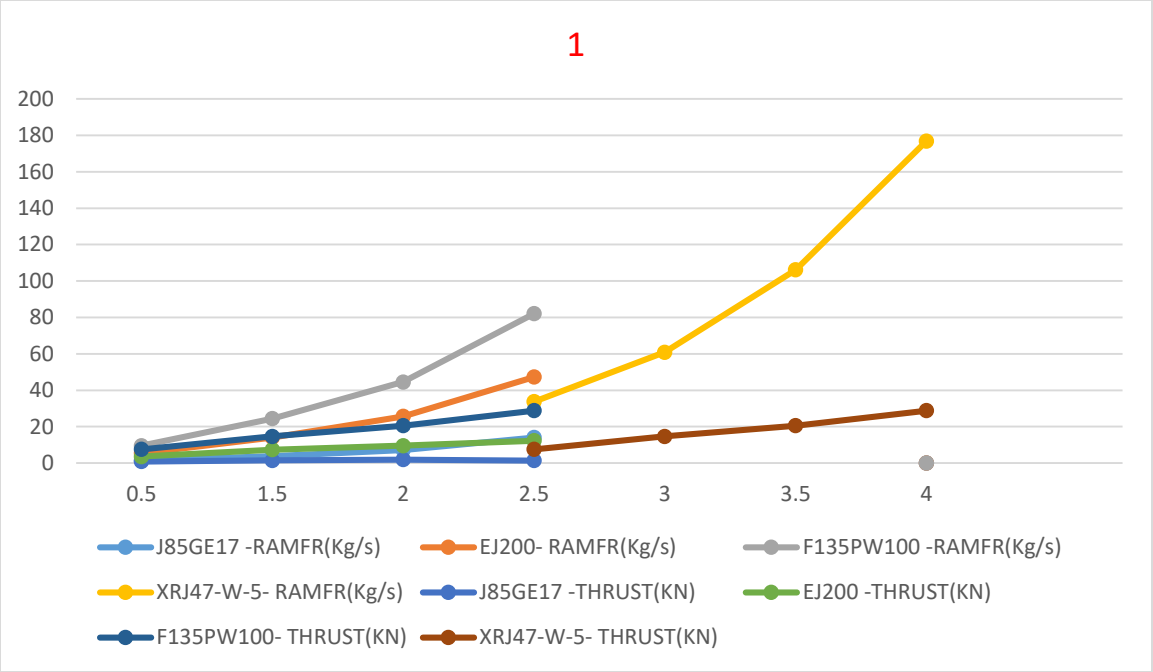

Figure 19 (9) Comparisons of the actual flow rate of the inlet air to the engine and thrust of the J85GE21 turbojet, F135 PW100 turbofan, EJ200 turbofan engines at an altitude of 20,000 meters and a Mach range of 0.5 to 2.5 and an XRJ47-W-5 engine at an altitude of 20,000 meters and a Mach range of 2.5 Up to 4 per JP10 fuel Also, the actual flow rates of the inlet air to the engine and thrust of J85GE17 turbojet, F135 PW100 turbofan, EJ200 turbofan, XRJ47-W-5 RAMJET engines, per mach, in the altitude range of 10,000-30,000 meters per JP10 fuel are shown in figure (). 19

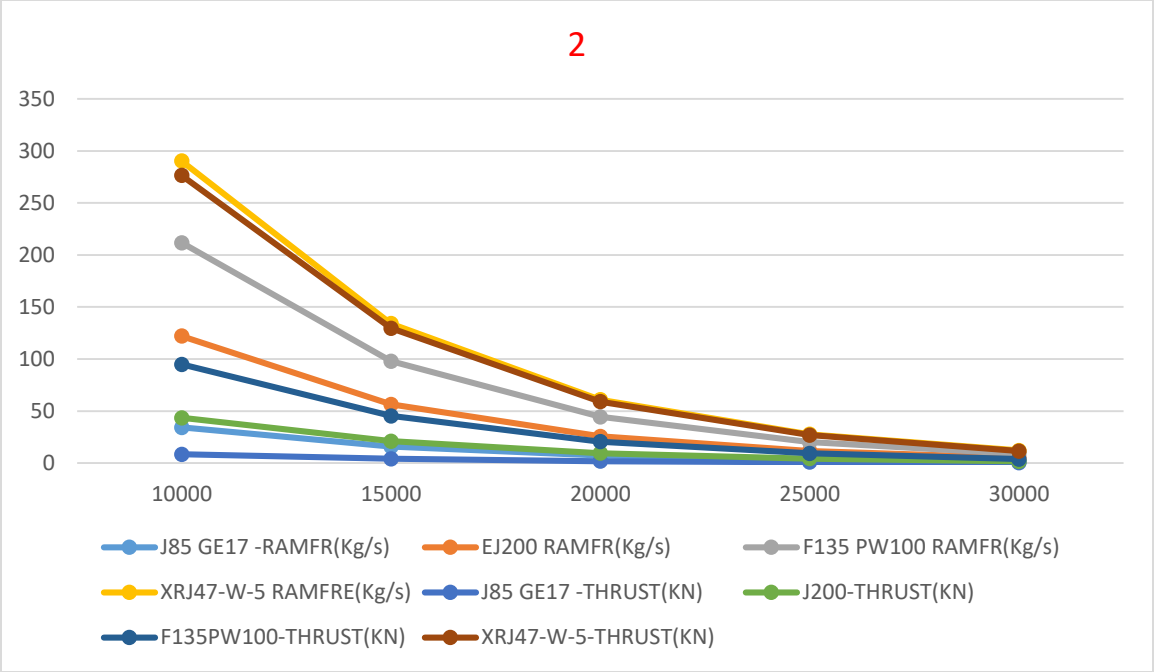

Fig. 20 () Actual flow rates of the inlet air to the engine and thrust of the J85GE17 turbojet, F135 PW100 turbofan, EJ200 turbofan, XRJ47-W-5 RAMJET engines, per Mach, in the altitude range of 10,000 to 30,000 meters, according to JP10 fuel. As the results show, for each constant Mach increase, the convection speed increases. According to the relation (), the increase in the convection speed leads to an increase in the actual flow rate of the incoming air. On the other hand, at any constant Mach, the density increases Ambient air is reduced. By reducing the density of the ambient air, the actual flow rate of the incoming air decreases. Also. For J85GE21 turbojet, F135 PW100 turbofan, EJ200 turbofan, XRJ47-W-5 ramjet engines at a constant altitude, the actual mass flow rate of the air entering the engine increases with the increase in Mach number. . At any constant Mach, with the increase in flight altitude, the actual flow rate of the incoming air should decrease, therefore the thrust force of the engine also decreases. 20

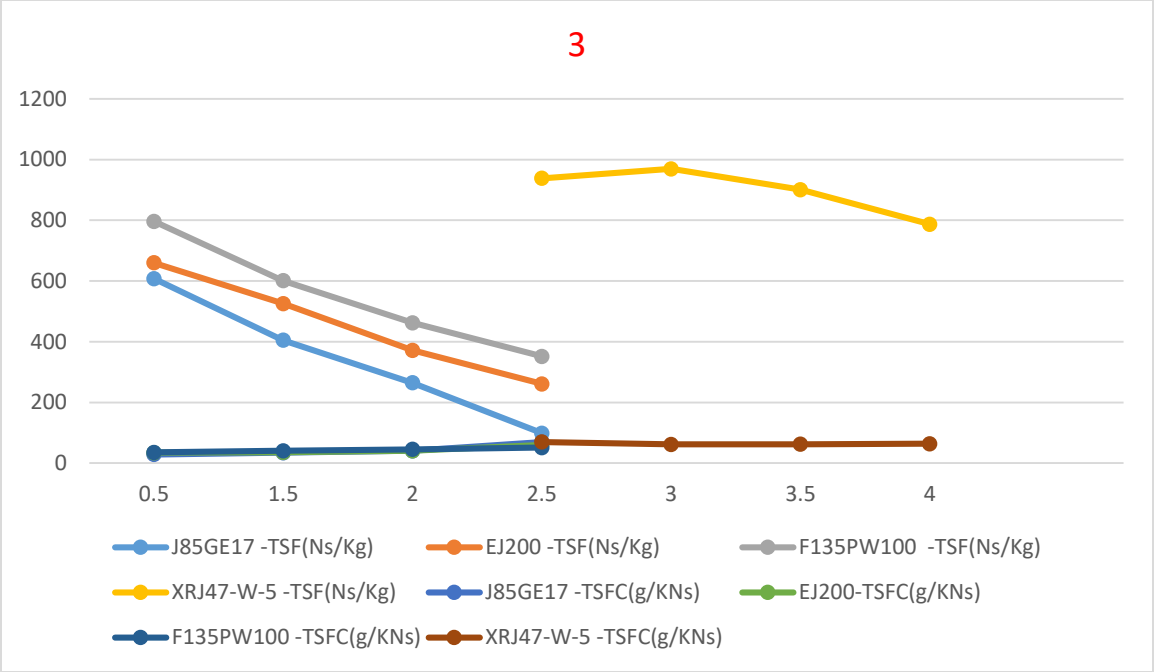

Figure 21: TSFC and TSF comparisons of J85GE21 turbojet engines, F135 PW100 turbofan, EJ200 turbofan, at an altitude of 20,000 meters and a range of Mach 0.5-2.5 and XRJ47-W-5 engine at an altitude of 20,000 meters and a range of Mach 2.5-4 per fuel JP10. Also, TSFC and TSF ratings of J85GE21 turbojet engines, F135 PW100 turbofan, EJ200 turbofan, at an altitude of 20,000 meters and a Mach range of 0.5 to 2.5 and XRJ47-W-5 engine at an altitude of 20,000 meters and a Mach range of 2.5 to 4 according to JP10 fuel. Figure () is displayed. 21

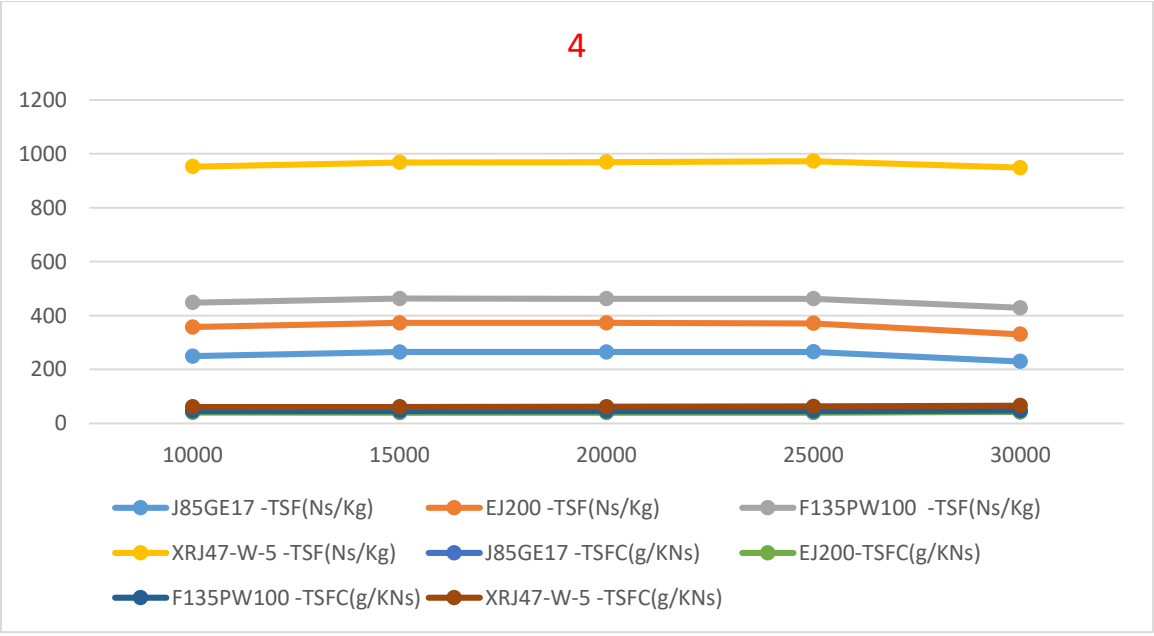

Figure 22: TSFC and TSF reductions for the J85GE17 turbojet, F135 PW100 turbofan, EJ200 turbofan, XRJ47-W-5 RAMJET engine and thrust engines, according to Mach 10,000 to 30,000 meters, according to fuel JP10.22

3-effect of fuel typeson performance

Thrust and TSFC comparisons at Mach 2 and cruising altitude of 10000 meters for F135PW100 engine for JP10, Natural gas and Hydrogen fuels are shown in figure (). 5- For JP10, Natural gas and Hydrogen fuels, it is shown in figure (). It has been observed that the molecular weight of combustion products with air (combustion productions) is also lower and with the decrease of molecular weight (molecular weight) of combustion products (combustion productions), the exit velocity from the nozzle (nozzle exit velocity) increases. As a result, the speed term of the thrust force increases. Therefore, the thermodynamic cycle has the highest thrust force for hydrogen fuel. Also, in equal conditions, with the increase in the calorific value of the fuel, the flow rate of the consumed fuel decreases, so the TSFC also decreases. Therefore, the lowest TSFC in the equal conditions belongs to the cycle with hydrogen fuel. On the other hand, with a decrease in molecular weight, under equal conditions, engine thrust increases, so TSF also increases. Therefore, per hydrogen cycle fuel, under equal conditions, it has the most TSF23.

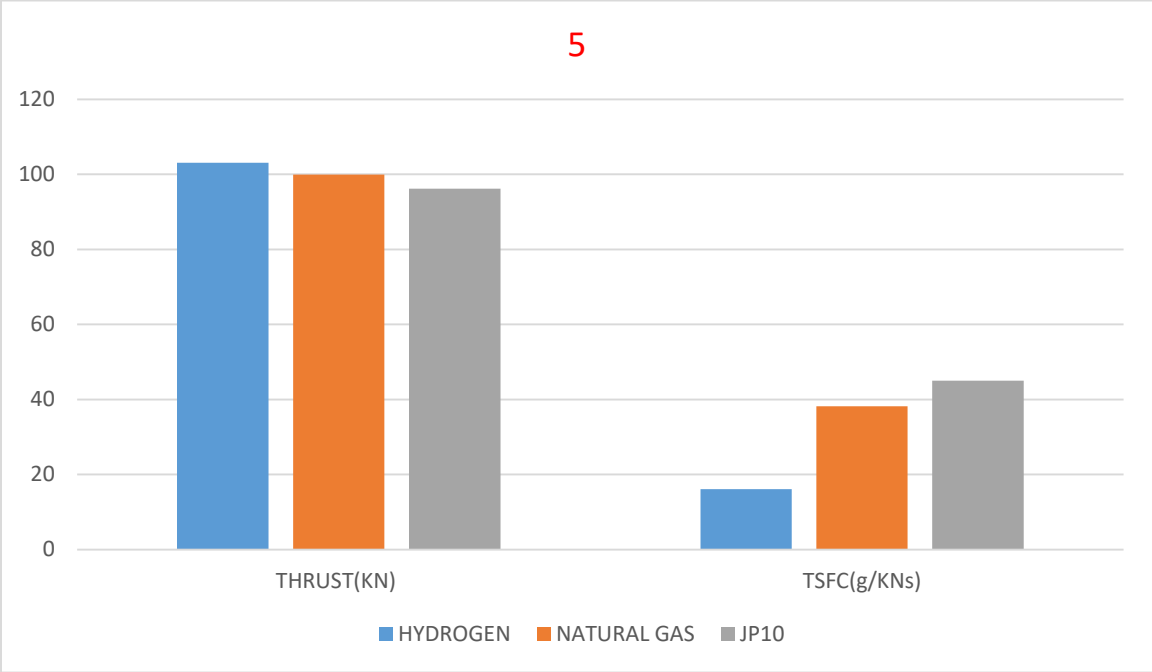

Fig. () Thrust and TSFC charts in the conditions of Mach 2 and altitude of 10000 meters for F135PW100 engine for JP10, Natural gas and Hydrogen fuels. 23

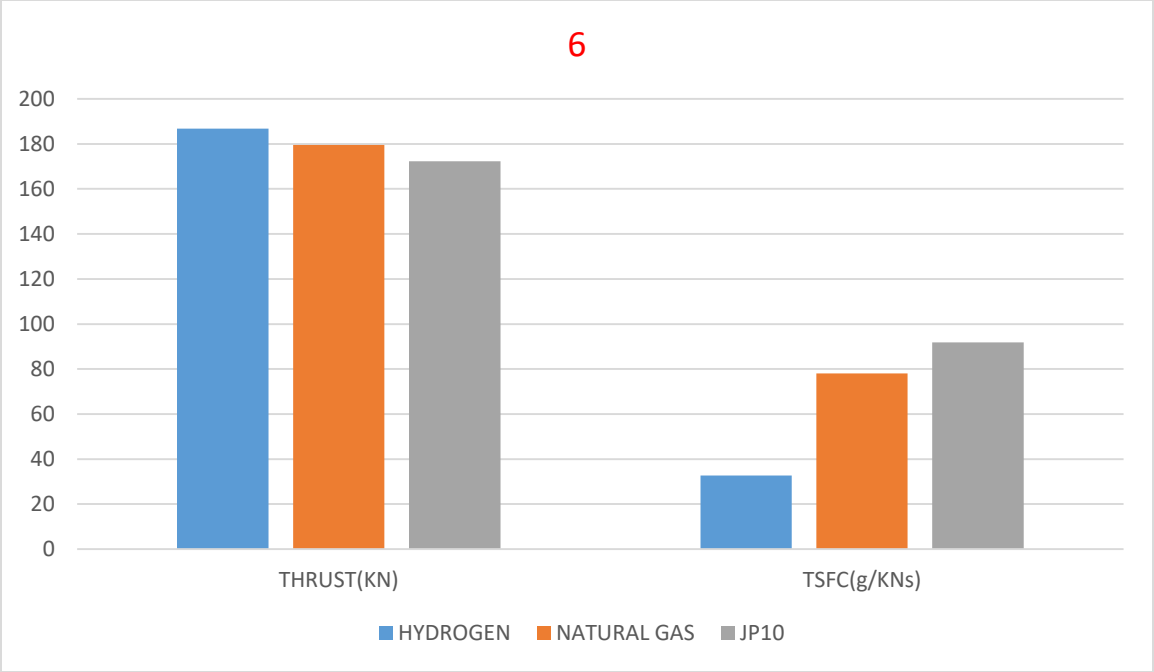

Figure () Thrust and TSFC charts in the conditions of Mach 3 and altitude of 10000 meters for XRJ47-W-5 engine for JP10, Natural gas and Hydrogen fuels.

3-Effect of inlet air temperature changes on performance

In this study, the effect of changes in inlet air temperature on J85GE21 turbojet, F135 PW100 turbofan, EJ200 turbofan, XRJ47-W-5 ramjet engines for using hydrogen and jet fuel at an altitude of 20000 meters and different Mach has been investigated. The changes of the inlet air flow rate for J85GE17 turbojet, F135 PW100 turbofan, EJ200 turbofan, XRJ47-W-5 ramjet engines at an altitude of 20,000 meters and for hydrogen fuel are shown in figure () for the inlet air temperature changes. J85GE17 turbojet, F135 PW100 turbofan, EJ200 turbofan, XRJ47-W-5 ramjet at any altitude and Mach, as the temperature of the inlet air decreases, the density of the inlet air increases, so the actual flow rate of the inlet air increases.24

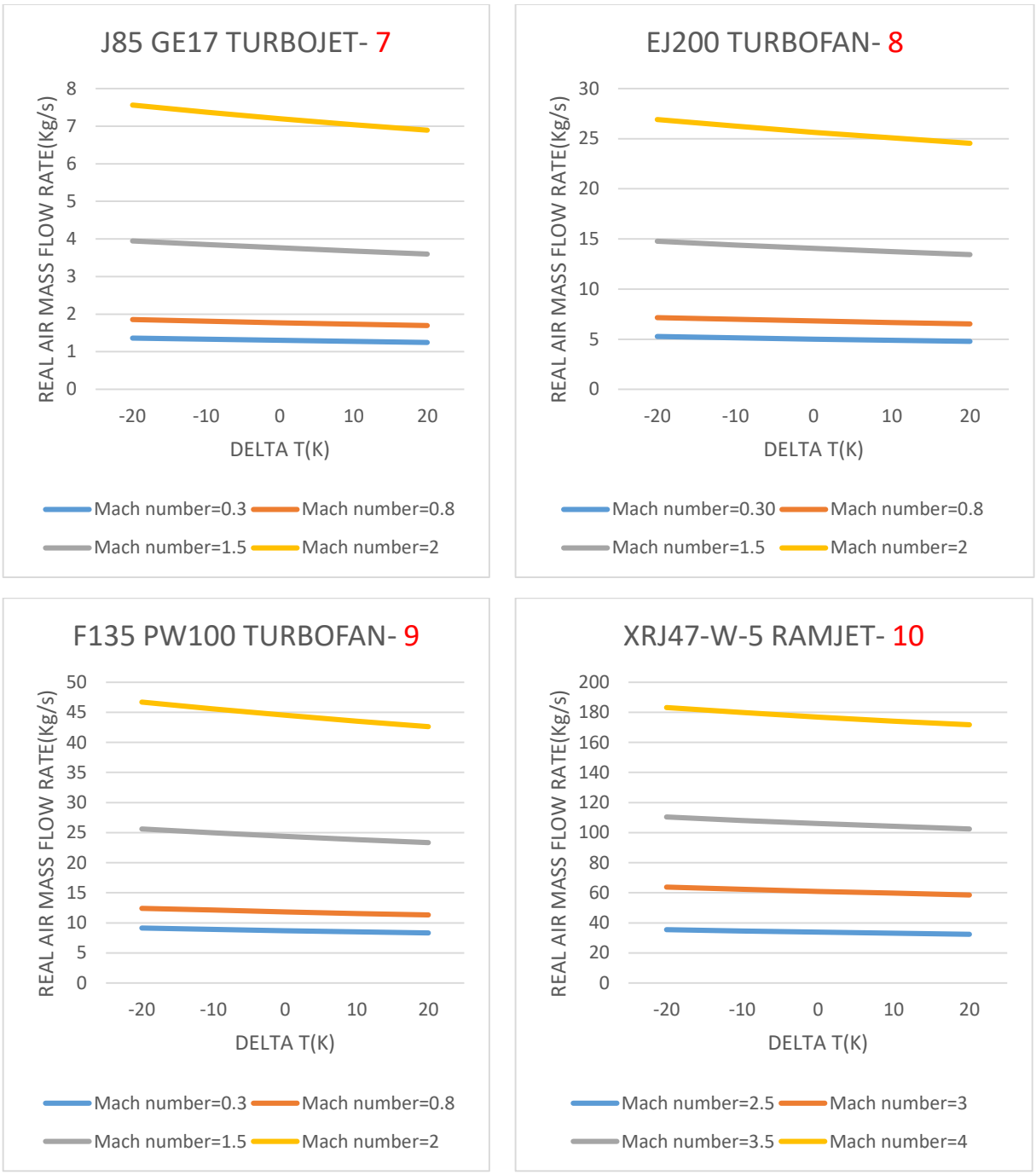

Figure 25: changes in the actual flow rate of the inlet air for J85GE17 turbojet, F135 PW100 turbofan, EJ200 turbofan, XRJ47-W-5 ramjet engines at an altitude of 20,000 meters and for hydrogen fuel Thrust changes for J85GE17 turbojet, F135 PW100 turbofan, EJ200 turbofan, XRJ47-W-5 ramjet engines at an altitude of 20,000 meters and for hydrogen fuel with changes in inlet air temperature are shown in figure (). For J85GE17 turbojet, F135 PW100 turbofan, EJ200 turbofan, XRJ47-W-5 ramjet engines, with the decrease of the inlet air temperature, the actual flow rate of the inlet air increases. Therefore, with the decrease of the inlet air temperature, the thrust of the engine also increases.25

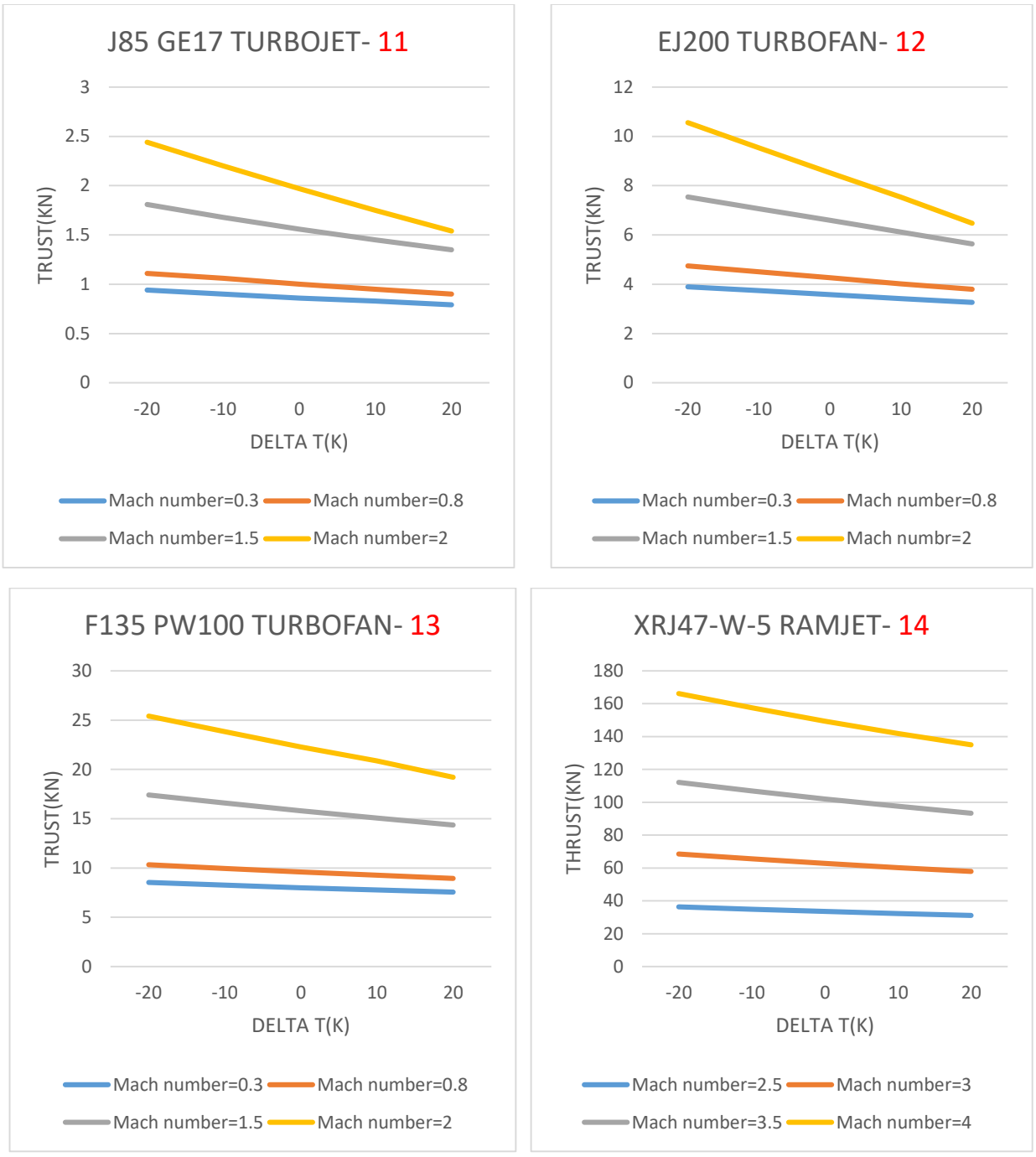

Figure 26: Thrust changes for J85GE17 turbojet, F135 PW100 turbofan, EJ200 turbofan, XRJ47-W-5 ramjet engines at an altitude of 20,000 meters and for hydrogen fuel with changes in inlet air temperature. Fuel flow rate changes for J85GE17 turbojet, F135 PW100 turbofan, EJ200 turbofan, XRJ47-W-5 ramjet engines at an altitude of 20,000 meters and for hydrogen fuel for J85GE17 turbojet, F135 PW100 turbofan, EJ200 turbofan, XRJ47-W-5 ramjet engines. It is shown in figure () with the changes of the inlet air temperature. Since the actual flow rate of the inlet air increases with the decrease of the inlet air temperature, more thermal energy is needed to

bring the flow temperature to the burner outlet temperature. Therefore, as the temperature of the intake air decreases, the fuel flow rate increases. 26

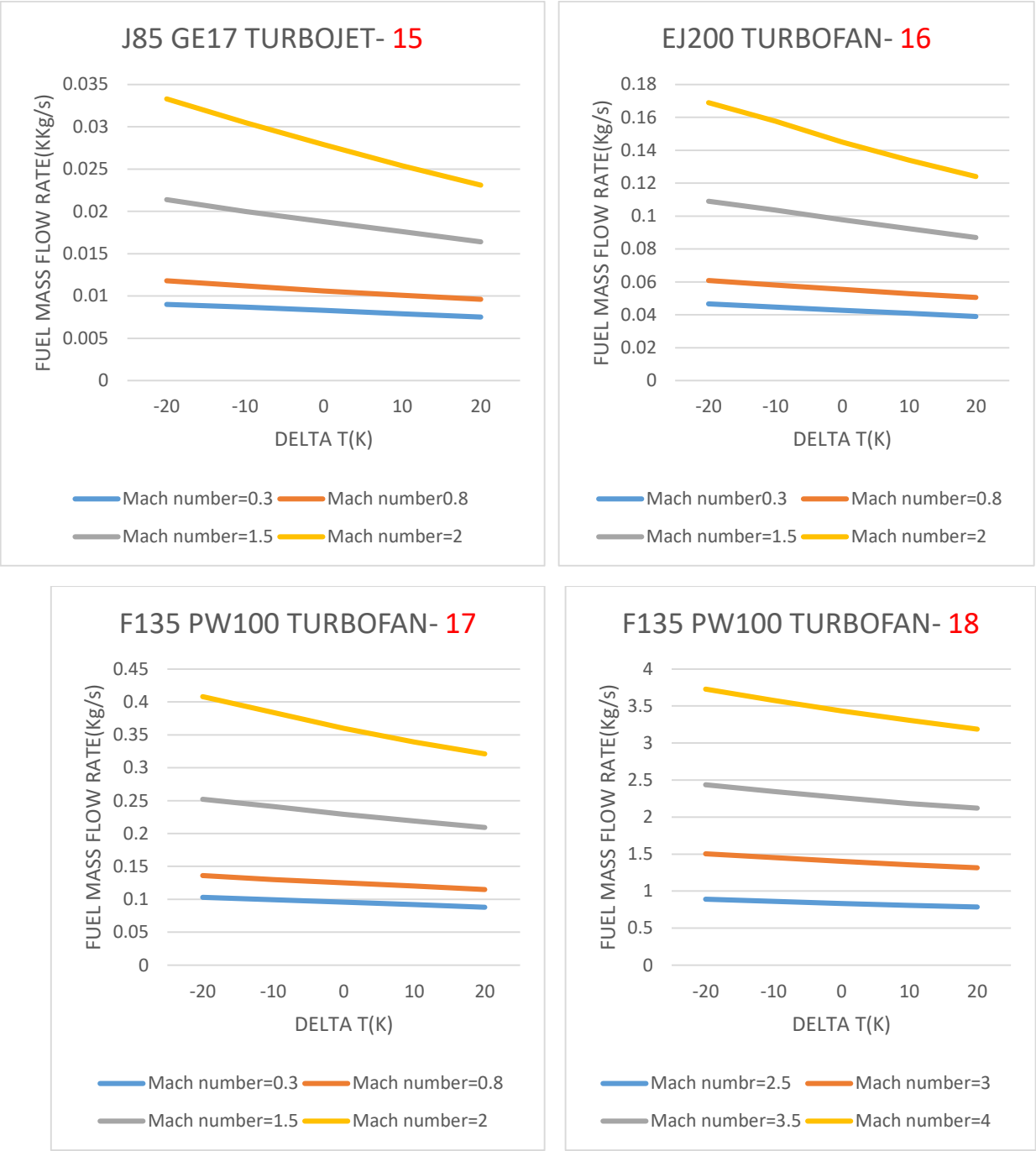

Figure 27 () changes in fuel consumption for J85GE17 turbojet, F135 PW100 turbofan, EJ200 turbofan, XRJ47-W-5 ramjet engines at an altitude of 20,000 meters and for hydrogen fuel with changes in inlet air temperature. TSFC changes for J85GE17 turbojet.F135 PW100 turbofan, EJ200 turbofan, XRJ47-W-5 ramjet engines at an altitude of 20,000 meters and for hydrogen fuel with changes in inlet air temperature are shown in figure (). For J85GE17 turbojet.F135 engines

PW100 turbofan, EJ200 turbofan, XRJ47-W-5 ramjet Since the increase in thrust force due to the decrease in intake air temperature is greater than the increase in fuel consumption due to the decrease in intake air temperature, therefore TSFC decreases with the decrease in intake air temperature. 27

Figure 28: TSFC changes for J85GE17 turbojet, F135 PW100 turbofan, EJ200 turbofan, XRJ47-W-5 ramjet engines at an altitude of 20,000 meters and for hydrogen fuel with changes in inlet air temperature. Thermal efficiency changes for J85GE17 turbojet engines, F135 PW100

turbofan, EJ200 turbofan, at an altitude of 20,000 meters and for hydrogen fuel with changes in inlet air temperature are shown in figure (). For J85GE17 turbojet engines, F135 PW100 turbofan, EJ200 turbofan, with a decrease in the temperature of the inlet air, the increase in the air flow rate (real inlet air mass flow rate...) is greater than the increase in the fuel mass flow rate (fuel mass flow rate...), so the changes in the kinetic energy of the flow along the engine with the rate The magnitude increases as the heating rate increases. Therefore, according to equation (), the thermal efficiency of the cycle increases with the decrease of inlet air temperature drop. 28

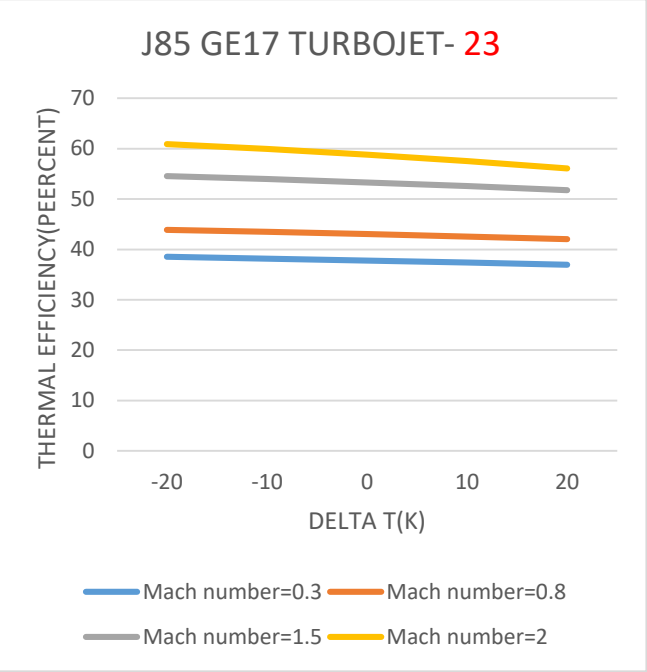

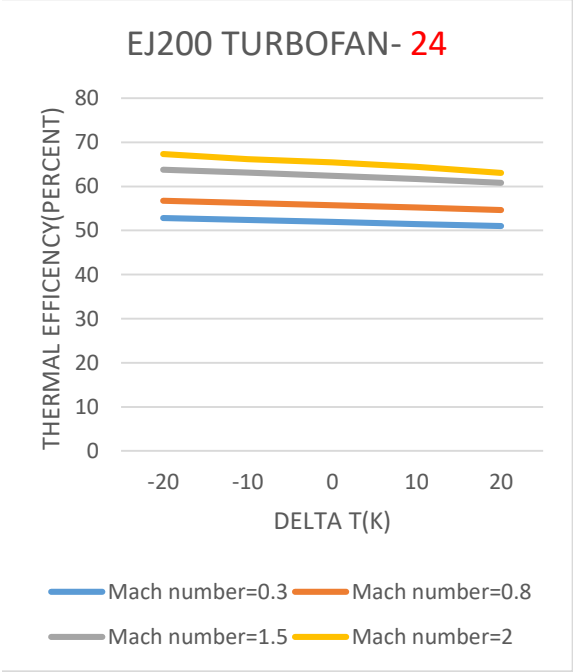

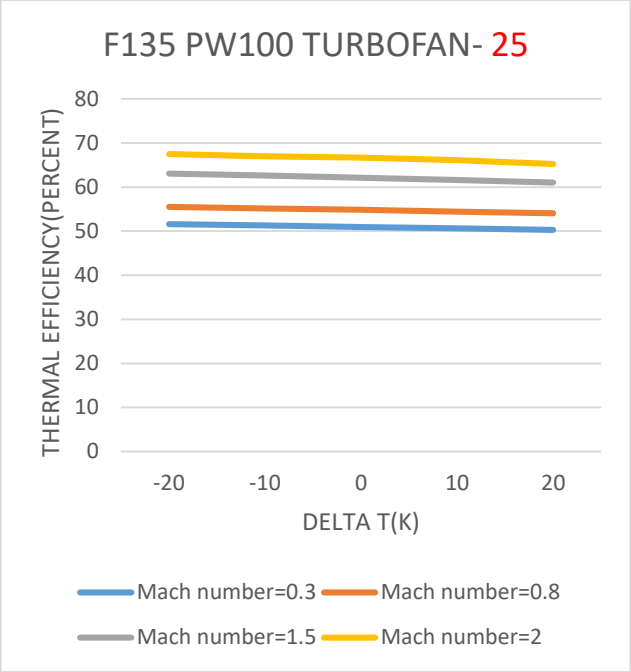

Figure 29: changes in thermal efficiency for J85GE17 turbojet engines, F135 PW100 turbofan, EJ200 turbofan, at an altitude of 20,000 meters and for hydrogen fuel with changes in inlet air temperature. Propulsion efficiency changes for J85GE17 turbojet engines, F135 PW100 turbofan, EJ200 turbofan, XRJ47-W-5 ramjet at an altitude of 20000 meters and for hydrogen fuel with changes in inlet air temperature are shown in figure (). For J85GE17 turbojet engines F135 PW100 turbofan, EJ200 turbofan, XRJ47-W-5 ramjet, as the temperature of the inlet air decreases, the propulsion efficiency decreases because the rate of increase in the thrust product in the cruising speed due to the decrease in the temperature of the inlet air is greater than the rate of increase in the kinetic energy of the flow along the engine. .29

Figure 30: Propulsion efficiency changes for J85GE17 turbojet, F135 PW100 turbofan, EJ200 turbofan, XRJ47-W-5 ramjet engines at an altitude of 20,000 meters and for hydrogen fuel with changes in inlet air temperature. The changes in the emission intensity of nitrogen oxides (EI nox) for J85GE17 turbojet engines, F135 PW100 turbofan, EJ200 turbofan, at an altitude of 20,000 meters and for hydrogen fuel with changes in inlet air temperature are shown in figure () for J85GE17 engines. turbojet. F135 PW100 turbofan, EJ200 turbofan, by reducing the inlet air temperature according to equation () EI nox is reduced.30

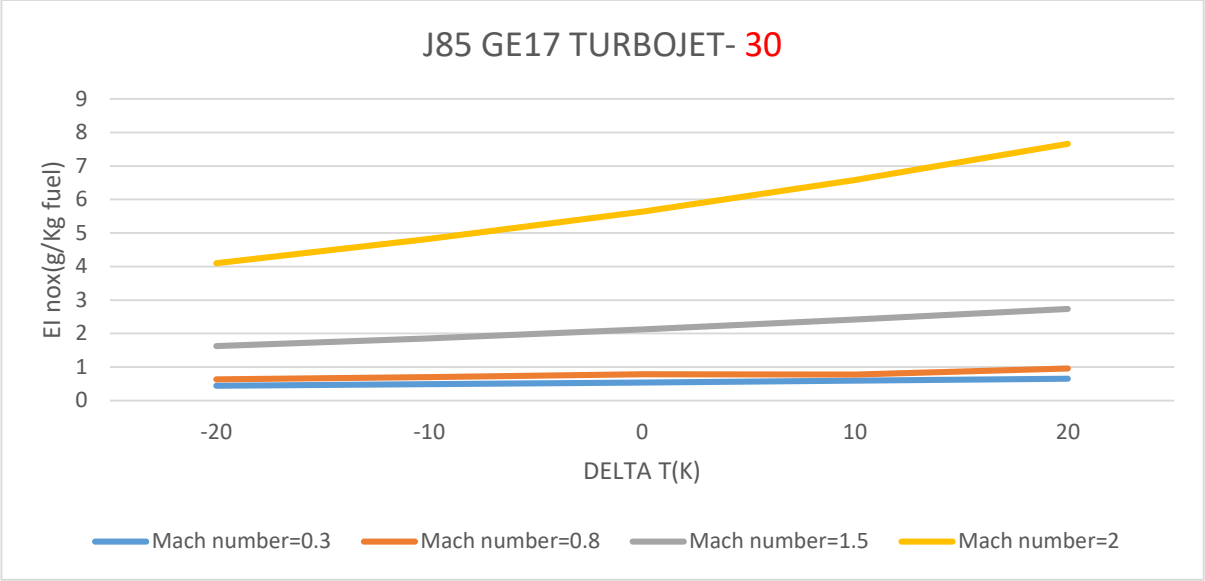
J85 GE17 TURBOJET- 30
EI nox(g/Kg fuel)
9
8
7
6
5
4
3
2
1
0
-20
-10
0
10
20
DELTA T(K)
Mach number=0.3
Mach number=0.8
Mach number=1.5
Mach number=2

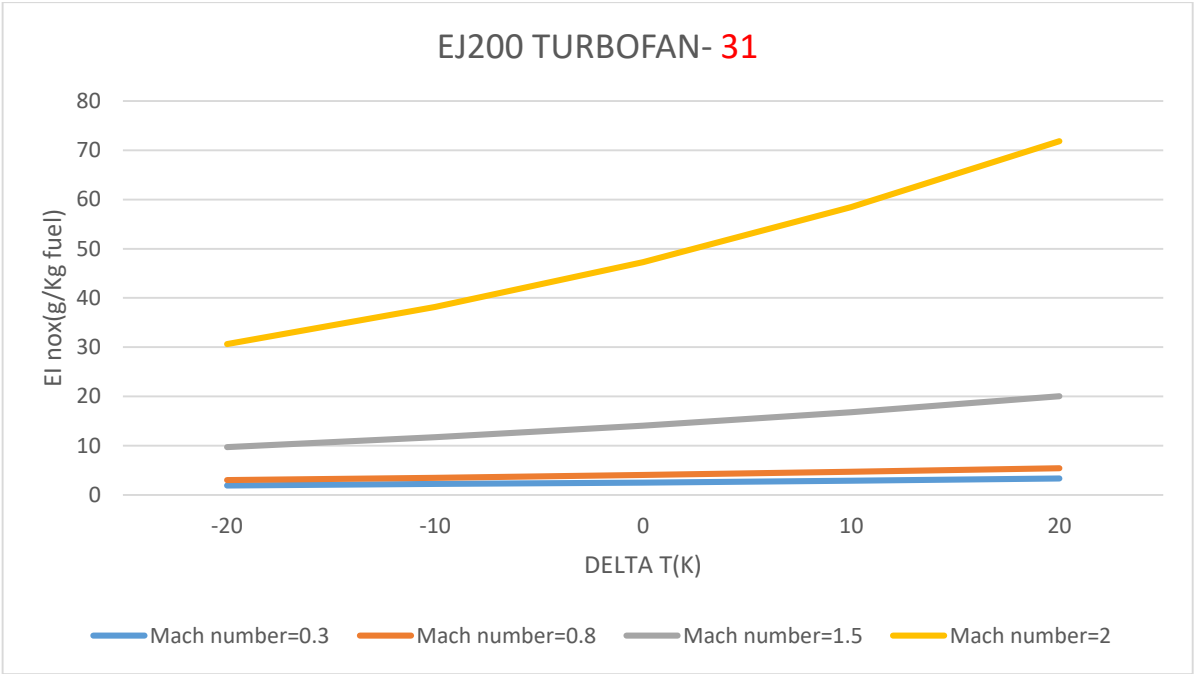
EJ200 TURBOFAN- 31
EI nox(g/Kg fuel)
80
70
60
50
40
30
20
10
0
-20
-10
0
10
20
DELTA T(K)
Mach number=0.3
Mach number=0.8
Mach number=1.5
Mach number=2

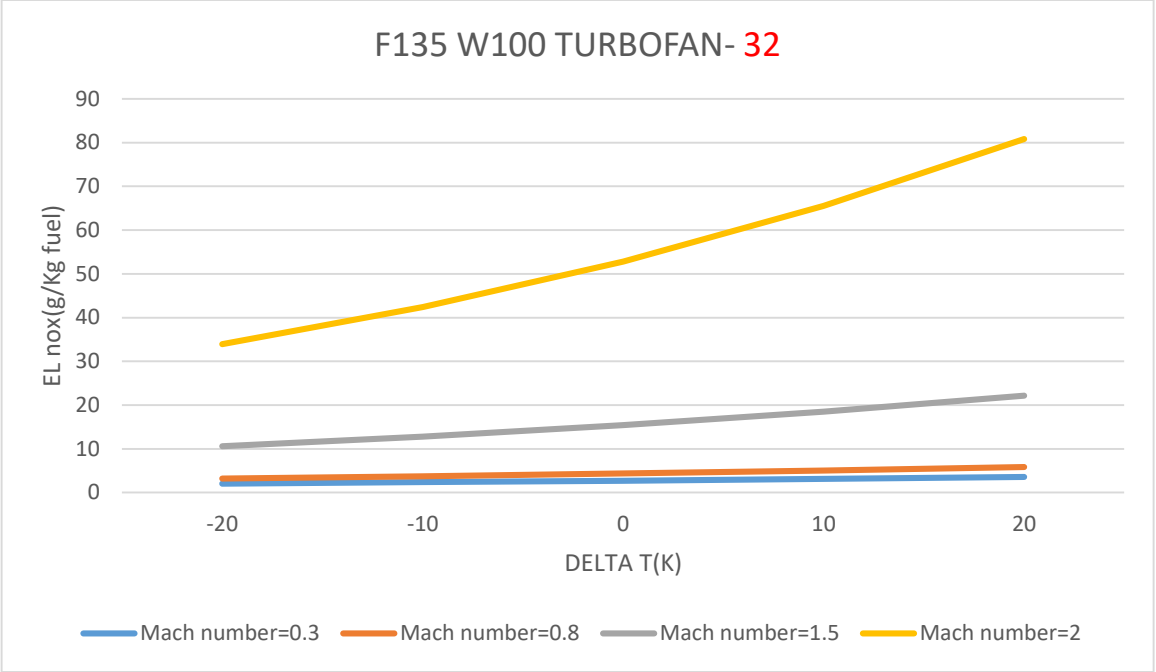

Figure 31 () changes in nitrogen oxide emission intensity (EI nox) for J85G17 turbojet engines, F135 PW100 turbofan, EJ200 turbofan, at an altitude of 20,000 meters and for hydrogen fuel with changes in inlet air temperature. 3- Intensity of influence of inlet air temperature on the performance of F135 PW100 turbofan, EJ200 turbofan, XRJ47-W-5 ramjet engines In this study, we have investigated the severity of the influence of inlet air temperature deviations on TSF and TSFC for XRJ47-W-5 ramjet engine, as well as EI nox and TSF deviations for F135 PW100 turbofan, EJ200 turbofan engines with Mach deviations. Comparisons of the desired parameters have been made in the two cases of TΔ=+10 and TΔ=-10 degrees Kelvin for different flight Machs at a flight altitude of 20,000 meters for hydrogen fuel. For the EJ200 turbofan engine, the percentage of TSF parameter deviations in TΔ=+10 and TΔ=-10 degrees Kelvin for different flight Machs at a flight altitude of 20,000 meters for hydrogen fuel at flight Machs of 0.3, 0.8, 1.5, and 2 respectively +4.41 and +6.57 and +10.06% and +20.86%. Also, the percentage of EI nox parameter deviations in the two conditions of TΔ=+10 and TΔ=-10 degrees Kelvin for different flight Machs at a flight altitude of 20,000 meters for hydrogen fuel at flight Machs of 0.3, 0.8, and 1 5 and 2 are -0.02, -25.98, -30.37 and -34.71%, respectively. For the F135 PW100 turbofan engine, the percentage of TSF parameter deviations in the two conditions of TΔ=+10 and TΔ=-10 degrees Kelvin for different flight Machs at a flight altitude of 20,000 meters to per hydrogen fuel at Mach 0.3, 0.8, 1.5, and 2 are +1.49, +2.57, +5.16, and +9.05%, respectively. Also, the percentage of EI nox parameter deviations in the two cases TΔ=+10 and TΔ=-10 degrees Kelvin per Different cruising Machs at the cruising altitude of 20,000 meters for hydrogen fuel at cruising Machs of 0.3, 0.8, 1.5, and 2 are -24.26, -26.36, -30.93, and -35.24%, respectively. Therefore, for F135 PW100, EJ200 turbofan engines, at a constant altitude, with an increase in the Mach number, the TSF increases with a larger pitch for a decrease in the inlet air temperature. Also, at a constant altitude, with an increase in the Mach number, the clearance for a decrease in the inlet air temperature EI nox increases with a pitch. The larger it is, the smaller it is. For the XRJ47-W-5 ramjet engine, the percentage of TSF parameter deviations in TΔ=+10

and TΔ=-10 degrees Kelvin for different cruising Machs at cruising altitude of 20,000 meters for hydrogen fuel at cruising Machs of 2.5, 3, 3.5, and 4 respectively + 3.54, +4.31, +5.53, and +7.39%. Also, the percentage of TSFC parameter deviations in TΔ=+10 and TΔ=-10 degrees Kelvin for different cruising Machs at a cruising altitude of 20,000 meters for hydrogen fuel at cruising Machs of 2.5 and 3 And 3.5 and 4 are -1.51, -1.62, -1.96 and -2.49%, respectively. Therefore, for the XRJ47-W-5 ramjet engine, at a constant altitude, with an increase in the Mach number, the TSF increases with a larger pitch for a decrease in the inlet air temperature. Also, at a constant height, with an increase in the Mach number, the clearance for a decrease in the inlet air temperature, TSFC, increases with a larger pitch. decreases.31

4)OPTIMIZATION

32

32 In this study, optimization for hydrogen fuel for three objective functions: 1-maximize TSF 2-minimize TSFC 3-maximize thermal efficiency in two separate phases 1- in the altitude range of 20,000 meters to 30,000 meters and the range of Mach 2-3 for J85GE17 turbojet engines. F135 PW100 turbofan, EJ200 turbofan and 3 to 4.5 for the XRJ47-W-5 ramjet engine and 2- for the cruise altitude range of 30,000 meters to 40,000 meters and the cruise Mach range of 2.5 to 3 for the J85GE17 turbojet engines. F135 PW100 turbofan, EJ200 turbofan and 3.5 to 4.5 for the XRJ47-W engine. -5 ramjets are done. 1-PHASE I In this phase, optimization has been done in the altitude range of 20,000 to 30,000 meters and the Mach range of 2 to 3 for J85GE17 turbojet engines, F135 PW100 turbofan, EJ200 turbofan and 3 to 4.5 for XRJ47-W-5 ramjet engines. Optimization parameters for J85GE17 turbojet, F135 PW100 turbofan, EJ200 turbofan and XRJ47-W-5 ramjet engines in PHASE1 conditions are shown in table (32).

Parameters	Limits	XRJ47-W-5 ramjet	F135 PW100 turbofan	EJ200 turbofan	J85 GE 17 TURBOJET
	Upper	2400	2200	2150	2000

Burner inlet temperature(k)	Lower	2000	1000	1000	1000
Compressor pressure ratio	Upper	-	30	30	15
	Lower	-	2	2	2
ΔT(k)	Upper	20	20	20	20
	Lower	-20	-20	-20	-20
Flight altitude(m)	Upper	30000	30000	30000	30000
	Lower	20000	20000	20000	20000
Flight Mach number	Upper	4.5	3	3	3
	Lower	3	2	2	2
Fan pressure ratio	Upper	-	6	6	-
	Lower	-	2	2	-
Design bypass ratio	Upper	-	10	10	-
	Lower	-	0.1	0.1	-

33. Optimization parameters for J85GE17 turbojet, F135 PW100 turbofan, EJ200 turbofan and XRJ47-W-5 ramjet engines. In PHASE1 conditions. Optimization constraints for J85GE21 turbojet, F135 PW100 turbofan, EJ200 turbofan and XRJ47-W-5 ramjet engines in PHASE1 conditions are shown in table (33).

Objective function	Parmeters	Limits	XRJ47-W-5 ramjet	F135 PW100 turbofan	EJ200 turbofan	J85 GE 17 TURBOJET
TSF	Thrust(KN)	Upper	50	45	25	10
		Lower	6	22.29	10.04	1.96
	TSFC(g/KNs)	Upper	25	17	15	15
		Lower	5	4	4	5
TSFC	Fuel mass flow rate(Kg/s)	Upper	0.850	0.370	0.160	0.030
		Lower	0.002	0.100	0.050	0.002
	TSF(Ns/Kg)	Upper	1500	700	500	500
		Lower	990	500	380	273
Thermal efficiency	TSF(Ns/Kg)	Upper	-	800	500	500
		Lower	-	495	385	450
	TSFC(g/KNs)	Upper	-	17	16	16
		Lower	-	4	2	5

Table 34: Optimization constraints for J85GE17 turbojet, F135 PW100 turbofan, EJ200 turbofan and XRJ47-W-5 ramjet engines in PHASE1 conditions. The optimal parameters for J85GE21 turbojet, F135 PW100 turbofan, EJ200 turbofan and XRJ47-W-5 ramjet engines for TSF maximization in PHASE1 conditions are shown in Table (34).

Parameters	XRJ47-W-5 ramjet	F135 PW100 turbofan	EJ200 turbofan	J85 GE 17 TURBOJET
Burner exit temperature(K)	2399	2122.71	1841	1595.31

Overall compressor pressure ratio	-	28.328	29.613	14.553
Fan pressure ratio	-	5.704	5.440	-
ΔT(K)	-19.94	-19.98	-19.54	-19.97
Design bypass ratio	-	0.102	0.102	-
Flight altitude(m)	21253	20749	21038.2	21597.6
Flight mach number	3	2.01	2	2

Table 35: Optimum parameters for J85GE17 turbojet, F135 PW100 turbofan, EJ200 turbofan and XRJ47-W-5 ramjet engines for TSF maximization in PHASE1 conditions. The optimal parameters for J85GE17 turbojet, F135 PW100 turbofan, EJ200 turbofan and XRJ47-W-5 ramjet engines for TSFC minimization in PHASE1 conditions are shown in table (35).

Parameters	XRJ47-W-5 ramjet	F135 PW100 turbofan	EJ200 turbofan	J85 GE 17 TURBOJET
Burner exit temperature(K)	2157.99	1775.46	1558.93	1196.3
Overall compressor pressure ratio	-	26.187	28.572	14.996
Fan pressure ratio	-	4.162	4.730	-
ΔT(K)	-19.99	-19.94	-19.78	-19.56
Design bypass ratio	-	0.130	0.114	-
Flight altitude(m)	22810.8	23308.5	21946	24718
Flight mach number	3.05	2	2	2

Table 36: Optimum parameters for J85GE17 turbojet, F135 PW100 turbofan, EJ200 turbofan, and XRJ47-W-5 ramjet engines to minimize TSFC in PHASE1 conditions The optimal parameters for J85GE17 turbojet, F135 PW100 turbofan, EJ200 turbofan and XRJ47-W-5 ramjet engines for maximizing thermal efficiency in PHASE1 conditions are shown in table (36).

Parameters	F135 PW100 turbofan	EJ200 turbofan	J85 GE 17 TURBOJET
Burner exit temperature(K)	2147.99	2149.99	1511.91
Overall compressor pressure ratio	29.941	29.948	14.998

Fan pressure ratio	5.951	5.700	-
ΔT(K)	-19.97	-19.98	-19.99
Design bypass ratio	0.419	0.939	-
Flight altitude(m)	20010.4	20008.2	21768
Flight mach number	2.240	2.241	2.084

Table 37. Optimum parameters for J85GE17 turbojet, F135 PW100 turbofan, EJ200 turbofan and XRJ47-W-5 ramjet engines for maximizing thermal efficiency in PHASE1 conditions. Performance of optimized cycles in PHASE1 The performance results of optimized cycles based on J85GE17 turbojet, F135 PW100 turbofan, EJ200 turbofan and XRJ47-W-5 ramjet engines with different objective functions in PHASE1 under design point conditions for hydrogen fuel have been investigated. A) J85 GE17 turbojet The performance results of the optimized cycles based on the J85 GE17 engine with different objective functions in the PHASE1 phase in the conditions of the design point for hydrogen fuel are shown in Table (37).

Objective function	Thrust(KN)	TSF(Ns/Kg)	Fuel mass flow rate(Kg/s)	TSFC	Propulsion efficiency(percent)	Thermal efficiency(percent)
TSF	3.12	531	0.046	14.997	67.85	67.64
TSFC	0.98	273.240	0.0137	13.173	80.15	68.35
Thermal efficiency	2.88	432.55	0.042	14.848	72.11	68.05

Table 38: performance results of optimized cycles based on the J85 GE17 engine with different objective functions in PHASE 1 under design point conditions for hydrogen fuel B) EJ200 turbofan The performance results of the optimized cycles based on the EJ200 turbofan engine with different objective functions in the PHASE1 phase in the conditions of the design point for hydrogen fuel are shown in table (38).

Objective function	Thrust(KN)	TSF(Ns/Kg)	Fuel mass flow rate(Kg/s)	TSFC	Propulsion efficiency(percent)	Thermal efficiency(percent)
TSF	12.40	543.263	0.186	14.994	67.62	67.82

TSFC	7.53	376.933	0.102	13.637	74.78	63.74
Thermal efficiency	13.98	386.87	0.223	15.991	76.70	70.88

Table 39: performance results of optimized cycles based on the EJ200 turbofan engine with different objective functions in PHASE 1 under design point conditions for hydrogen fuel C). F135 PW100 turbofan The performance results of the optimized cycles based on the F135 PW100 turbofan engine with different target functions in PHASE 1 under design point conditions for Hydrogen fuel are shown in Table (39).

Objective function	Thrust(KN)	TSF(Ns/Kg)	Fuel mass flow rate(Kg/s)	TSFC	Propulsion efficiency(percent)	Thermal efficiency(percent)
TSF	28.66	690.219	0.487	16.998	62.29	67.53
TSFC	13.87	500.216	0.208	15.037	69.37	65.75
Thermal efficiency	31.06	495.849	0.223	16.998	71.99	69.82

Table 40: Performance results of optimized cycles based on F135 PW100 turbofan engine with different objective functions in PHASE 1 under design point conditions for hydrogen fuel D) XRJ47-W-5 ramjet. The performance results of the optimized cycles based on the XRJ47-W-5 ramjet engine with different target functions in PHASE 1 under design point conditions for Hydrogen fuel are shown in Table (40).

Objective function	Thrust(KN)	TSF(Ns/Kg)	Fuel mass flow rate(Kg/s)	TSFC	Propulsion efficiency(percent)
TSF	60	1138.446	1.387	23.113	60.86
TSFC	40.49	990.045	0.847	20.926	63.91

Table () performance results of optimized cycles based on XRJ47-W-5 ramjet engine with different objective functions in PHASE 1 under design point conditions for hydrogen fuel 2-PHASE2 In this phase, optimization has been done in the cruising altitude range of 30,000 meters to 40,000 meters and the cruising Mach range of 2.5 to 3 for J85GE21 turbojet engines, F135 PW100 turbofan, EJ200 turbofan and 3 to 4.5 for XRJ47-W-5 ramjet engines. Optimization parameters for J85GE21 turbojet, F135 PW100 turbofan, EJ200 turbofan, and XRJ47-W-5 ramjet engines in PHASE2 conditions are shown in table (41).

Objective function	Parameters	Limits	XRJ47-W-5 ramjet	F135 PW100 turbofan	EJ200 turbofan	J85 GE 21 TURBOJET
TSF	Thrust(KN)	Upper	30	20	10	5
		Lower	18	4.85	1.38	0.22
	TSFC(g/KNs)	Upper	25	26	28	30
		Lower	5	4	5	5
TSFC	Fuel mass flow rate(Kg/s)	Upper	0.500	0.125	0.040	0.007
		Lower	0.050	0.001	0.001	0.002
	TSF(Ns/Kg)	Upper	1000	600	500	500
		Lower	930	296	146	75
Thermal efficiency	TSF(Ns/Kg)	Upper	-	600	500	150
		Lower	-	295	150	55
	TSFC(g/KNs)	Upper	-	24	26	34
		Lower	-	5	5	5

Table () optimization parameters for J85GE21 turbojet, F135 PW100 turbofan, EJ200 turbofan and XRJ47-W-5 ramjet engines in PHASE2 conditions The optimization constraints for J85GE21 turbojet, F135 PW100 turbofan, EJ200 turbofan and XRJ47-W-5 ramjet engines in PHASE2 conditions are shown in table (42).

Objective function	Parameters	Limits	XRJ47-W-5 ramjet	F135 PW100 turbofan	EJ200 turbofan	J85 GE 21 TURBOJET
TSF	Thrust(KN)	Upper	30	20	10	5
		Lower	18	4.85	1.38	0.22
	TSFC(g/KNs)	Upper	25	26	28	30
		Lower	5	4	5	5
TSFC	Fuel mass flow rate(Kg/s)	Upper	0.500	0.125	0.040	0.007
		Lower	0.050	0.001	0.001	0.002
	TSF(Ns/Kg)	Upper	1000	600	500	500
		Lower	930	296	146	75
Thermal efficiency	TSF(Ns/Kg)	Upper	-	600	500	150
		Lower	-	295	150	55
	TSFC(g/KNs)	Upper	-	24	26	34
		Lower	-	5	5	5

Table () optimization constraints for J85GE21 turbojet, F135 PW100 turbofan, EJ200 turbofan and XRJ47-W-5 ramjet engines in PHASE2 conditions The optimal parameters for J85GE21 turbojet, F135 PW100 turbofan, EJ200 turbofan and XRJ47-W-5 ramjet engines for TSF maximization in PHASE2 conditions are shown in table (43).

	XRJ47-W-5 ramjet	F135 PW100 turbofan	EJ200 turbofan	J85 GE 21 TURBOJET
Burner exit temperature(K)	2400	2199.97	2149.86	1999.97
Overall compressor pressure ratio	-	2.026	2.091	2
Fan pressure ratio	-	5.682	3.983	-
ΔT(K)	-19.96	-19.62	-19.58	-19.97
Design bypass ratio	-	0.100	0.100	-
Flight altitude(m)	30006	30023.5	30016.6	30025
Flight mach number	3.500	2.501	2.500	2.504

Table () optimal parameters for J85GE21 turbojet, F135 PW100 turbofan, EJ200 turbofan and XRJ47-W-5 ramjet engines for TSF maximization in PHASE2 conditions. The optimal parameters for J85GE21 turbojet, F135 PW100 turbofan, EJ200 turbofan and XRJ47-W-5 ramjet engines for TSFC minimization in PHASE2 conditions are shown in table (44).

	XRJ47-W-5 ramjet	F135 PW100 turbofan	EJ200 turbofan	J85 GE 21 TURBOJET
Burner exit temperature(K)	2222.19	1789.75	1709.48	1611.93
Overall compressor pressure ratio	-	17.773	14.912	11.183
Fan pressure ratio	-	5.687	4.922	-
ΔT(K)	-19.98	-19.98	-19.99	-19.78
Design bypass ratio	-	0.100	0.108	-
Flight altitude(m)	30001.1	30009.3	32173.4	35774.3
Flight mach number	3.500	2.503	2.500	2.500

Table () of optimal parameters for J85GE21 turbojet, F135 PW100 turbofan, EJ200 turbofan and XRJ47-W-5 ramjet engines to minimize TSFC in PHASE2 conditions The optimal parameters for J85GE21 turbojet, F135 PW100 turbofan, EJ200 turbofan and XRJ47-W-5 ramjet engines for maximizing thermal efficiency in PHASE2 conditions are shown in table (45).

	F135 PW100 turbofan	EJ200 turbofan	J85 GE 21 TURBOJET
Burner exit temperature(K)	2167.90	2147.18	1997.49
Overall compressor pressure ratio	11.291	9.827	10.075
Fan pressure ratio	5.910	4.143	-
ΔT(K)	-19.97	-19.99	-19.99
Design bypass ratio	0.175	0.100	-
Flight altitude(m)	30005.3	30002	30000.7
Flight mach number	2.911	2.999	2.998

Table of optimal parameters for J85GE21 turbojet, F135 PW100 turbofan, EJ200 turbofan and XRJ47-W-5 ramjet engines for maximizing thermal efficiency in PHASE2 conditions.
Performance of optimized cycles in PHASE2 Performance results of optimized cycles based on J85GE21 turbojet, F135 PW100 turbofan, EJ200 turbofan, and XRJ47-W-5 ramjet engines with different objective functions in PHASE2 under design point conditions for hydrogen fuel have been investigated.

A)J85 GE17 turbojet

The performance results of the optimized cycles based on the J85 GE17 engine with different objective functions in PHASE 2 under design point conditions for Hydrogen fuel are shown in Table (46).

Objective function	Thrust(KN)	TSF(Ns/Kg)	Fuel mass flow rate(Kg/s)	TSFC	Propulsion efficiency(percent)	Thermal efficiency(percent)
TSF	1.99	677.220	0.045	22.631	68.54	58.25
TSFC	0.35	292.860	0.0069	6.645	83.66	68.32
Thermal efficiency	2.22	389.690	0.054	24.496	81.77	74.33

Table () performance results of optimized cycles based on J85 GE17 engine with different objective functions in PHASE 2 under design point conditions for hydrogen fuel

B) EJ200 turbofan

The performance results of the optimized cycles based on the EJ200 turbofan engine with different objective functions in the PHASE2 phase in the conditions of the design point for Hydrogen fuel are shown in Table (47).

Objective function	Thrust(KN)	TSF(Ns/Kg)	Fuel mass flow rate(Kg/s)	TSFC	Propulsion efficiency(percent)	Thermal efficiency(percent)
TSF	6.48	659.139	0.154	23.858	69.41	54.13
TSFC	2.05	292.689	0.040	19.505	83.58	60.41
Thermal efficiency	7.38	415.143	0.184	24.995	69.70	69.70

Table () performance results of optimized cycles based on EJ200 turbofan engine with different objective functions in PHASE 2 in design point conditions for hydrogen fuel

C) .F135 PW100 turbofan

The performance results of the optimized cycles based on the F135 PW100 turbofan engine with different target functions in PHASE 2 under design point conditions for Hydrogen fuel are shown in Table (48).

Objective function	Thrust(KN)	TSF(Ns/Kg)	Fuel mass flow rate(Kg/s)	TSFC	Propulsion efficiency(percent)	Thermal efficiency(percent)
TSF	11.54	676.356	0.284	24.607	68.89	51.95
TSFC	5.74	335.829	0.109	19.047	81.39	63.77
Thermal efficiency	11.50	412.926	0.276	24.048	80.72	68.48

Table () performance results of optimized cycles based on F135 PW100 turbofan engine with different objective functions in PHASE2 phase in design point conditions. For Hydrogen fuel

D) XRJ47-W-5 ramjet.

The performance results of the optimized cycles based on the XRJ47-W-5 ramjet engine with different target functions in PHASE 2 under design point conditions for hydrogen fuel are shown in Table ().

49

Objective function	Thrust(KN)	TSF(Ns/Kg)	Fuel mass flow rate(Kg/s)	TSFC	Propulsion efficiency(percent)
TSF	23.17	1048.770	0.551	23.8787	67.17
TSFC	20.56	930.218	0.448	21.826	69.62

Table () performance results of optimized cycles based on XRJ47-W-5 ramjet engine with different objective functions in PHASE2 phase in design point conditions. For Hydrogen fuel

Analysis of optimization results Among the cycles optimized in PHASE 1 and PHASE 2, the highest propulsion efficiency in the conditions of the design point of the cycle belongs to the optimized cycle based on J85 GE17 based on the minimization of TSFC in PHASE 2. Also, the highest TSF and the lowest TSFC in the conditions of the design point respectively belong to the optimized cycles based on Based on XRJ47-W-5 based on TSF maximization in PHASE1 phase, the optimized vehicle is based on J85E17 based on TSFC minimization in PHASE2 phase.50 5) Cycles selection In this study, among the optimized cycles based on J85GE21 turbojet, F135 PW100 turbofan, EJ200 turbofan gas turbine engines in PHASE I and PHASE II, hydrogen fuel was selected with two approaches and one cycle for each approach in each phase. Selection criteria for optimized cycles in PHASE I and 2 respectively, Thermal efficiency (percent) SDF(KN/pa) Propulsive efficiency(percent) TSFC(g/KNs) TSF is (Ns/Kg). In this study, for the optimized cycles in both phases, selection was made with two approaches: Energy consumption and environmental and Power and maneuverability. The weight coefficients of Energy consumption and environmental and Power and maneuver ability approaches are shown in table ().

	TSF	TSFC	Propulsive efficiency	cd	Thermal efficiency	EI nox
Energy consumption and environmental	0	-0.85	0	0	+0.95	-0.90
Power and maneuver ability	+0.90	0	+0.85	+0.95	0	0

Table () weighting coefficients of Energy consumption and environmental and Power and maneuver ability approaches. The points obtained by the optimized cycles in PHASE1 in the

Energy consumption and environmental and Power and maneuver ability approaches are shown in figure ().52

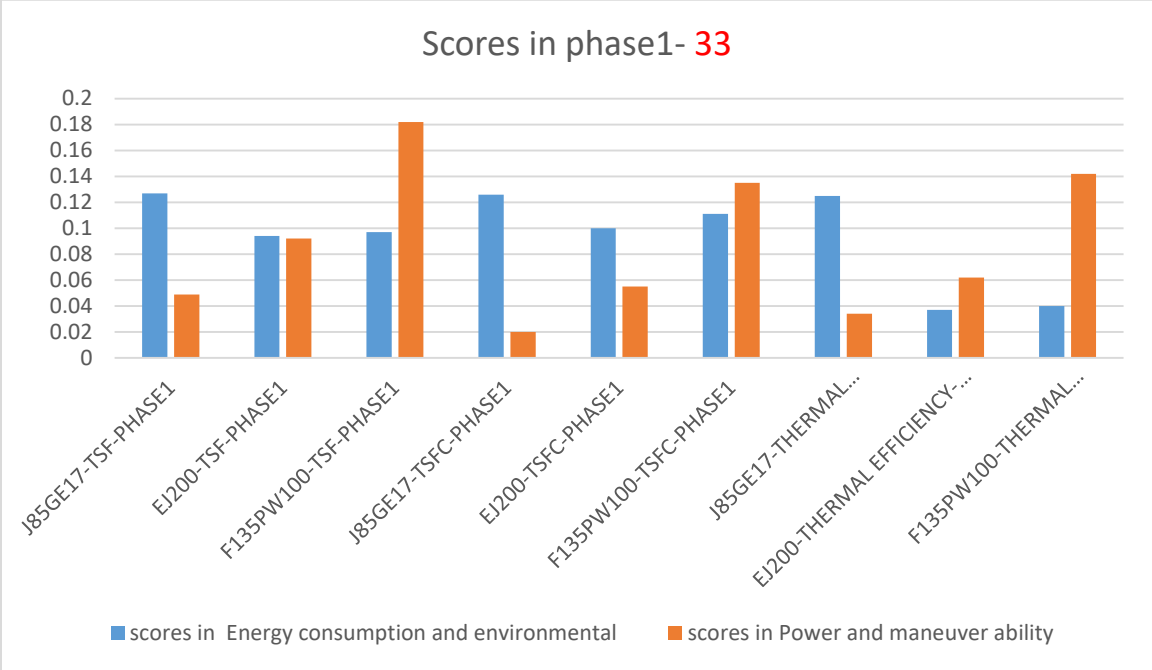

Figure () Score obtained by optimized cycles in PHASE1 in Energy consumption and environmental and Power and maneuver ability approaches. Therefore, in PHASE 1, with the Energy consumption and environmental approach, the optimized cycle based on J85GE17 based on TSF maximization has scored the highest and the optimized cycle based on EJ200 based on Thermal efficiency maximization has scored the lowest. Therefore, the optimized cycle based on J85GE17 based on TSF maximization in PHASE 1 and with Energy consumption and environmental approach was chosen. Also, in PHASE1 phase with Power and maneuverability approach, the optimized cycle based on F135PW100 based on TSF maximization has the highest score and the optimized cycle based on J85GE17 and for minimizing TSFC has obtained the lowest score. Therefore, the optimized cycle based on F135PW100 based on TSF maximization was selected in PHASE 1 with the Power and maneuverability approach. The entropy temperature diagram of the optimized cycle based on J85GE17 based on TSF maximization and the optimized cycle based on F135PW100 based on TSF maximization under design point

conditions are shown in figures () and () respectively. 53

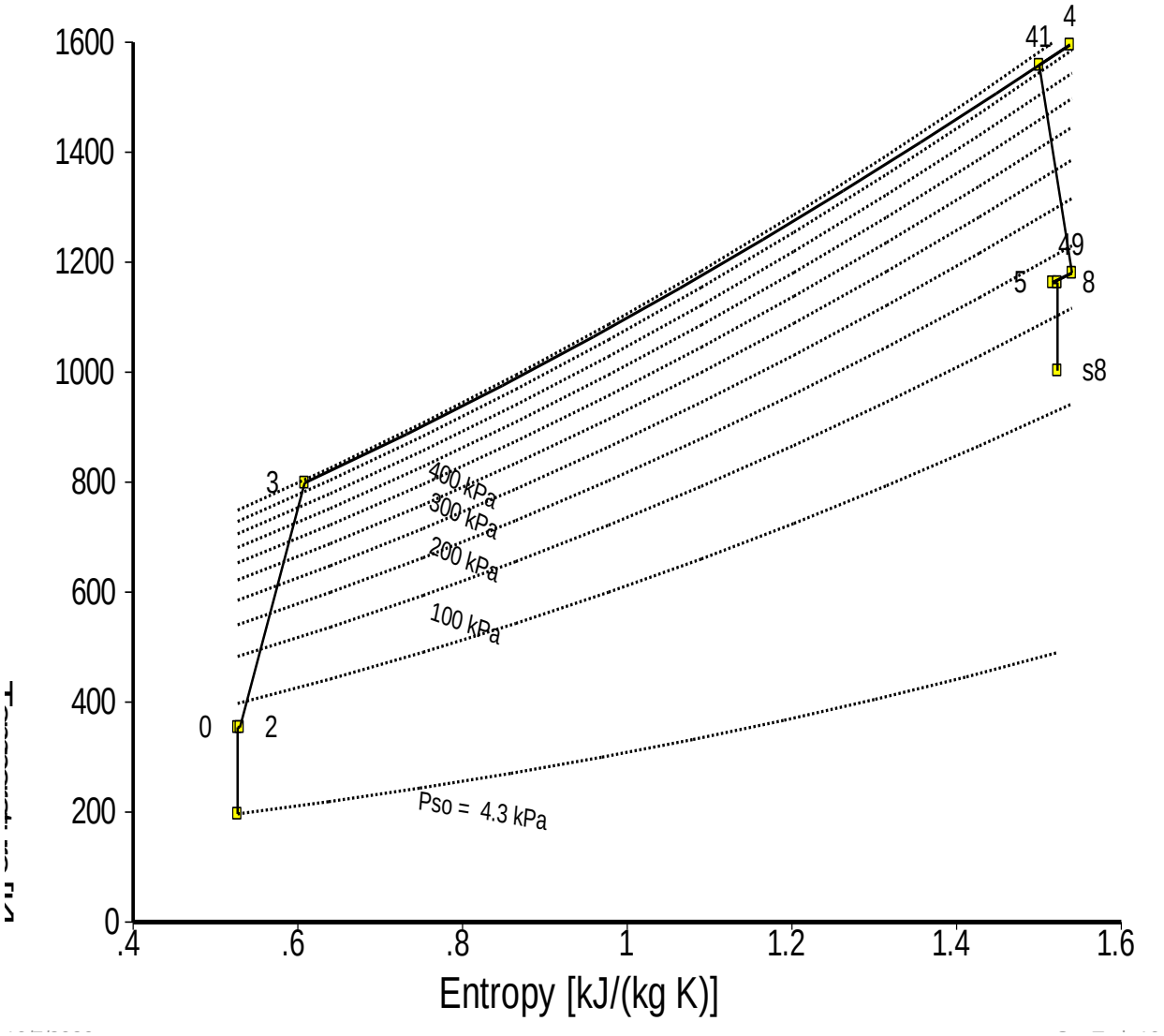

Figure () temperature diagram of optimized entropy cycle based on J85GE17 based on TSF maximization in design point conditions

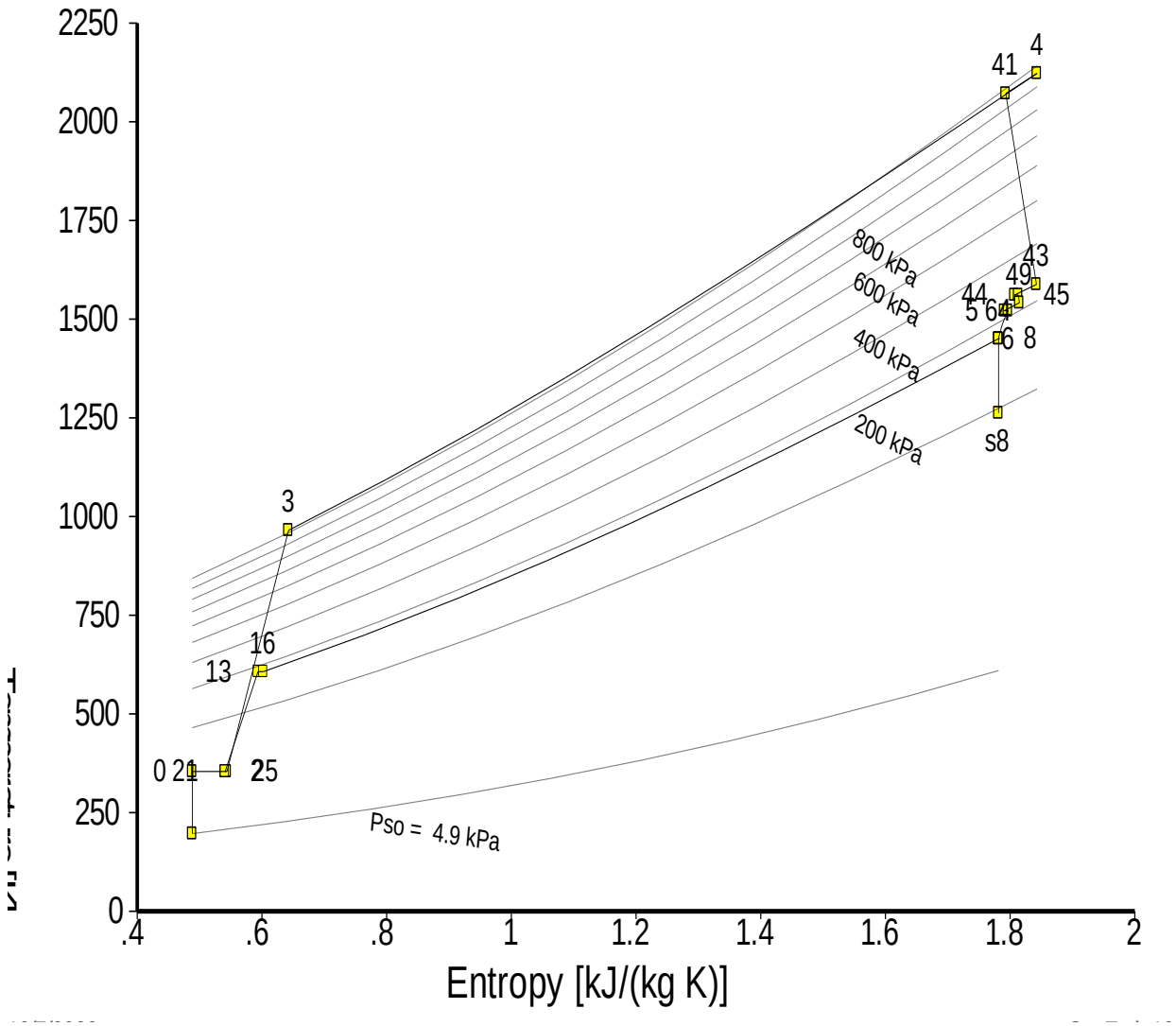

Temperature diagram of optimized entropy cycle based on F135PW100 based on TSF maximization in design point conditions. The points obtained by the optimized cycles in PHASE2 in the Energy consumption and environmental and Power and maneuver ability

approaches are shown in figure (54).

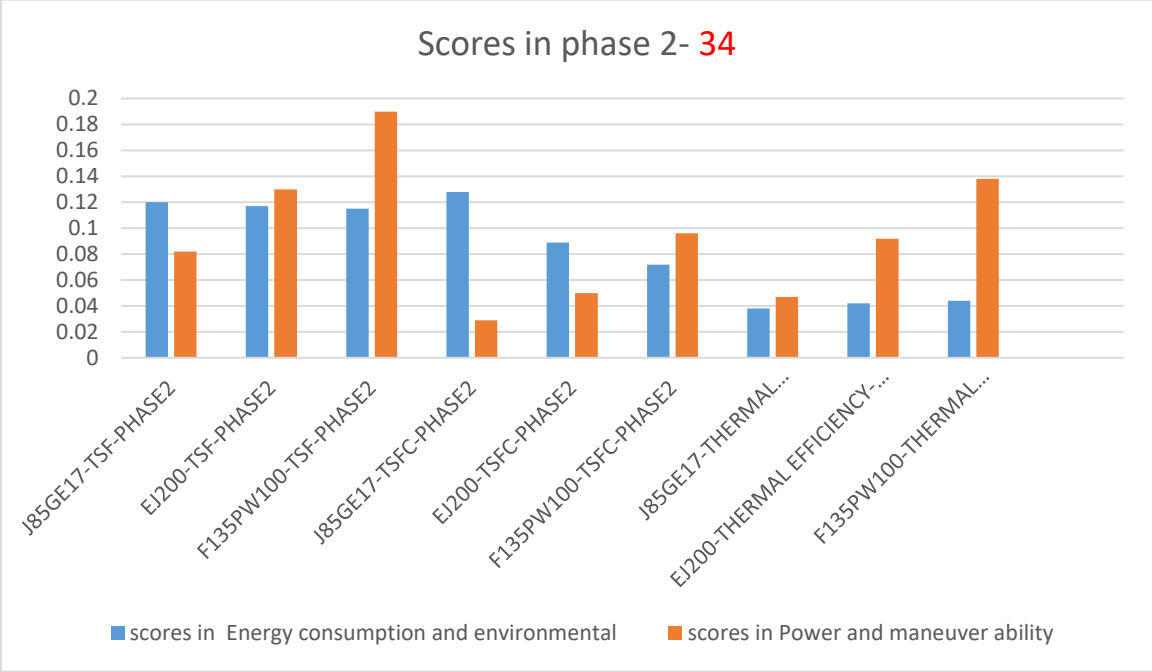

Figure () Score obtained by optimized cycles in PHASE2 in Energy consumption and environmental and Power and maneuver ability approaches.

Therefore, in PHASE 2, with the Energy consumption and environmental approach, the optimized cycle based on J85GE17 based on TSFC minimization has scored the highest and the optimized cycle based on J85GE17 based on Thermal efficiency maximization has scored the lowest. Therefore, the optimized cycle based on J85GE17 based on TSFC minimization in PHASE 2 and with the Energy consumption approach and environmental was selected. Also, in PHASE2 phase with the Power and maneuverability approach, the cycle optimized based on F135PW100 based on TSF maximization has scored the highest and the cycle optimized based on J85GE17 based on TSFC minimization has scored the lowest. Therefore, the optimized cycle based on F135PW100 based on TSF maximization has scored the lowest PHASE 2 was selected with the Power and maneuverability approach. The entropy temperature diagram of the optimized cycle based on J85GE17 based on TSFC minimization and the optimized cycle based on F135PW100 based on TSF maximization under design point conditions are shown in figures

() and () respectively. 55

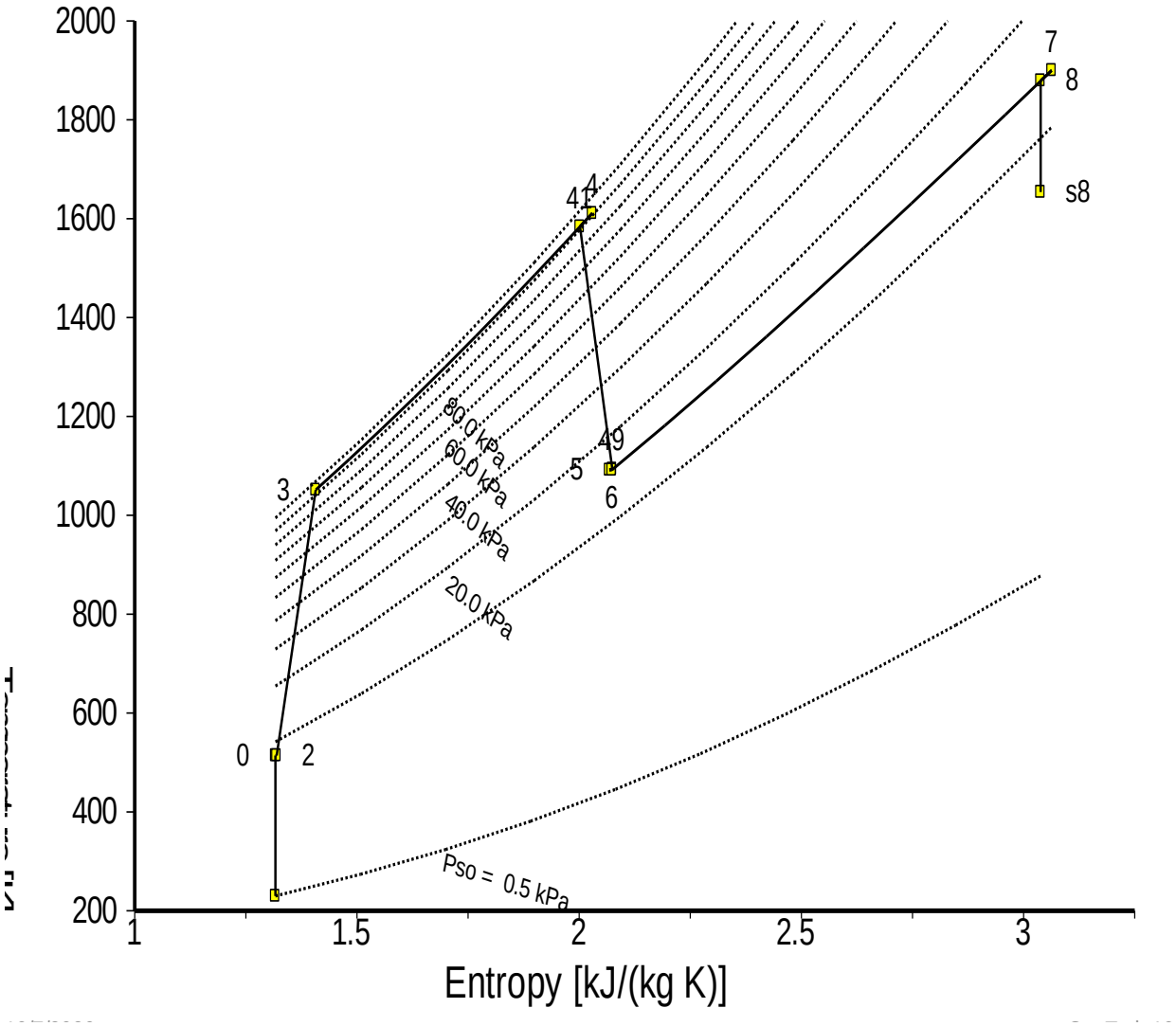

Optimized cycle entropy temperature diagram based on J85GE17 based on TSFC minimization in design point conditions

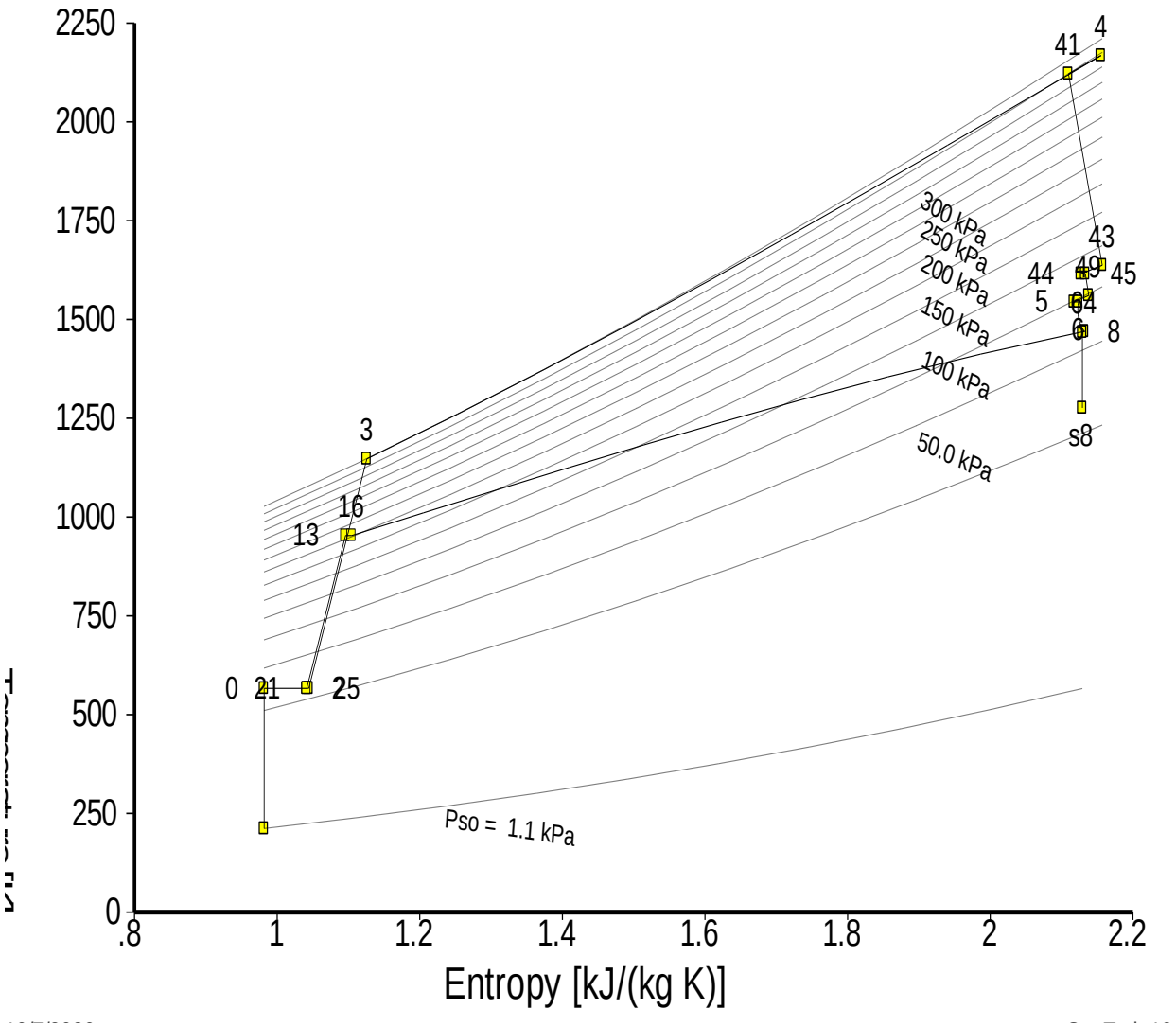

Temperature diagram of optimized entropy cycle based on F135PW100 based on TSF maximization in design point conditions. Comparison of the performance parameters of the selected cycles in the situation outside the design point

The comparison of the performance parameters of the cycles selected in PHASE 1 in the condition of Ma=2.4 and H=27000m for JP10 and Hydrogen fuels is shown in table ().56

Cycle	Fuel type	TSF(Ns/Kg)	TSFC(g/KNs)	Fuel mass flow rate(Kg/s)	Thermal efficiency(percent)	Propulsive efficiency(percent)

F135 - TSF	Hydrogen	527.486	18.687	0.243	69.07	72.46
	JP10	491.889	52.342	0.636	65.374	74.57
J85 - TSF	Hydrogen	371.280	17.221	0.026	70.13	78.51
	JP10	354.570	48.904	0.072	67.05	79.80

Table (comparison of the performance parameters of the selected cycles in PHASE 1 in the state of Ma=2.4 and H=27000m). For JP10 and Hydrogen fuels

The comparison of the performance parameters of the cycles selected in PHASE 2 in the state of Ma=3 and H=33000m for JP10 and Hydrogen fuels is shown in table ().57

Cycle	Fuel type	TSF(Ns/Kg)	TSFC(g/KNs)	Fuel mass flow rate(Kg/s)	Thermal efficiency(percent)	Propulsive efficiency(percent)
F135 - TSF	Hydrogen	541.940	27.971	0.292	58.42	77.27
	JP10	501.528	78.863	0.763	54.92	79.75
J85 - TSFC	Hydrogen	124.560	32.994	0.014	68.19	93.20
	JP10	113.120	98.387	0.039	64.54	94.11

Table (comparison of the performance parameters of the selected cycles in PHASE 2 in the state of Ma=3 and H=33000m). For JP10 and Hydrogen fuels

CONCLUSIONS

In the present study, the effect of Mach and take-off altitude of ramjet XRJ47-W-5 air engines, F135PW100 and EJ200 turbofan engines, and J85 GE17 turbojet on performance parameters of thrust and specific fuel consumption (TSFC) and fuel consumption and thermal efficiency. The engine has been checked. The specific results of the surveys are summarized below: 1. For turbofan engines F135PW100 and EJ200 and turbojet J85 GE17 and XRJ47-W-5 ramjet, with an increase in Mach, thrust and flow rate, fuel consumption, thermal efficiency, propulsion efficiency, tsfc increases and TSF decreases. 2. In this study, the effect of inlet air temperature changes on ramjet XRJ47-W-5 air engines and F135PW100 and EJ200 turbofan engines and J85 GE17 turbojet on performance parameters of thrust and specific fuel consumption (TSFC) and fuel consumption and thermal efficiencies and the thrust and intensity of nitrogen oxides emission (EI nox) and the actual flow rate of the air entering the engine were investigated. For the turbofan engines F135PW100 and EJ200, turbojet J85 GE17 and Ramjet XRJ47-W-5, by reducing the temperature of the air intake, the trust and TSF and flow rate of fuel consumption and thermal efficiency increase and tsfc and propulsion efficiency decrease. Also, by reducing the inlet air temperature, EI nox for F135PW100 and EJ200 turbofan engines and J85 GE17 turbojet is reduced.59 3. 60 Also, in this

study, the effect of Mach Bravazi on the intensity of the influence of the inlet air temperature variations on the performance of XRJ47-W-5 Ramjet air engines, F135PW100 and EJ200 turbofan engines, and J85 GE17 turbojet engines was investigated. For the XRJ47-W-5 Ramjet engine With the increase of Mach number, the intensity of increase in TSF and decrease in TSFC due to the decrease in inlet air temperature increases. Also, for F135PW100 and EJ200 turbofan engines and turbojet J85 GE17, with the increase in Mach number, the intensity of decrease in EI nox and increase in TSF due to decrease in inlet air temperature increases. finds.60 4. 61 Also, the type of fuel type on thrust and TSFC of ramjet XRJ47-W-5 air engines and turbofan engines F135PW100 and EJ200 and turbojet J85 GE17 were investigated. Increasing the calorific value of the fuel leads to a decrease in the flow of consumed fuel and a decrease in TSFC. Also, reducing the molecular weight of the fuel leads to an increase in thrust. Therefore, among the studied fuels, the use of hydrogen fuel brings the lowest TSFC and the highest thrust. 61 5. 62 The best optimal mode using TOPSIS decision making method in PHASE 1 and PHASE 2 with Energy consumption and environmental approach respectively belongs to the optimized cycle based on J85GE17 and based on maximizing TSF and the optimized cycle based on J85GE17 based on minimizing TSFC. 6. The best optimal mode using TOPSIS decision-making method in PHASE 1 and PHASE 2 with Power and maneuverability approach belongs to the optimized cycle based on F135 PW100 and based on TSF maximization.